Remote Sensing of Environment 148 (2014) 28–41

Contents lists available at ScienceDirect

Remote Sensing of Environment

journal homepage: www.elsevier.com/locate/rse

Estimation of water-related biochemical and biophysical vegetation properties using multitemporal airborne hyperspectral data and its comparison to MODIS spectral response

A. Casas [a,*], D. Riaño [a,b,e], S.L. Ustin [a], P. Dennison [c], J. Salas [d,e]

[a] Department of Land, Air, and Water Resources, University of California, One Shields Avenue, Davis, CA 95616, USA
[b] Centro de Ciencias Humanas y Sociales, Consejo Superior de Investigaciones Científicas, Albasanz 26-28, 28037 Madrid, Spain
[c] Department of Geography and Center for Natural and Technological Hazards, University of Utah, 270 S Central Campus Dr, Rm 270, Salt Lake City, UT 84112, USA
[d] Department of Geography and Geology, University of Alcalá, Calle Colegios 2, 28801 Alcalá de Henares, Spain
[e] Associated Research Unit GEOLAB b and d.

ARTICLE INFO

Article history:
Received 15 August 2013
Received in revised form 5 March 2014
Accepted 8 March 2014
Available online xxxx

Keywords:
Advanced Visible Infrared Imaging Spectrometer (AVIRIS)
Moderate Resolution Imaging Spectrometer (MODIS)
Foliar water content
Canopy water content
Fuel moisture content
Leaf mass per area
Leaf area index
Vegetation indexes
Curve-fitting
PROSAIL

ABSTRACT

Vegetation biochemical and biophysical parameters related to water are pivotal to understanding the water cycle and its interactions with carbon and energy balance. This study assessed a wide range of methods to estimate foliar water content (FWC, g/cm^2), canopy water content (CWC, g/cm^2), fuel moisture content (FMC) and interrelated variables leaf mass per area (LMA, g/cm^2), foliar biomass (FB, g/m^2), and leaf area index (LAI, m^2/m^2) using multitemporal Airborne Visible Infrared Imaging Spectrometer (AVIRIS) data. Estimations are compared to in-situ measurements stratified by cover type (i.e. grasses, shrubs and forest) made at Stanford University's Jasper Ridge Biological Preserve, California, USA. Curve-fitting techniques, a widely accepted method to retrieve CWC from AVIRIS, proved relatively inaccurate. Standard and recently designed vegetation indexes (VIs) provided higher accuracy; however, the most accurate VI differed by variable and by cover types. To evaluate if a hyperspectral narrow band sensor enhances the retrieval of these variables over multispectral broad bands, AVIRIS was convolved to Moderate Resolution Imaging Spectroradiometer (MODIS) bands. Best band combination indexes out of all possible bands improved the retrievals significantly over VI in the case of FMC, LMA and FB using AVIRIS bands in the longer SWIR wavelength region. AVIRIS PROSAIL and MODIS CWC PROSAIL radiative transfer model inversion had difficulty retrieving three of these variables simultaneously without a precise knowledge of the remaining chemical and physical conditions of the vegetation and soil. The SWIR region must be further investigated for water retrievals given that soil, dry mass and water are interrelated in the spectral signal plus the additional unknown impact of canopy structure upon the spectrum.

1. Introduction

Monitoring and predicting changes in the water content of vegetation cover are of major importance to agricultural and ecological understanding due to the key role of water on transpiration and carbon gain through stomatal regulation, hence determining interactions between the carbon, water, energy and nitrogen cycles (Cowan, 1982; Schulze & Hall, 1982; Ustin, Riano, & Hunt, 2012). Remote sensing is a unique tool for providing information linked to biochemical and biophysical characteristics of vegetation at multitemporal and spatial scales (Fourty & Baret, 1997; Ustin, Roberts, Gamon, Asner, & Green, 2004). Different quantities and methods measure the amount of water in foliage (Hunt, Ustin, & Riaño, 2013). Table 1 summarizes these water-related variables and their acronyms. FWC represents approximately 66% of leaf fresh mass averaged over a large number of leaf types (Jacquemoud et al., 1996). LMA is mainly composed of cellulose, lignin, protein, starch and minerals. LMA is a leaf trait strongly related positively to both temperature and leaf longevity and negatively to precipitation (Wright, Reich, Cornelissen, Falster, Garnier, et al., 2005; Wright, Reich, Cornelissen, Falster, Groom, et al., 2005; Wright et al., 2004) and related to strategies for assimilation, respiration and evapotranspiration, hence relevant for modeling carbon cycle, identification of functional types, seasonality or leaf turnover rate (Kokaly, Asner, Ollinger, Martin, & Wessman, 2009). FB affects photosynthetic rates, respiration rates and nutrient content (Reich et al., 1999). CWC has important implications for biochemical cycling in agriculture, forestry and natural ecosystems and relates to the water cycle through fine scale impacts like water deficit stress and forest physiology (Ustin et al., 2012). Finally, FMC is used in fire science to determine wildfire ignition probability and influences fire spread rates, providing critical information for wildfire risk assessment (Yebra et al., 2013).

* Corresponding author.

http://dx.doi.org/10.1016/j.rse.2014.03.011
0034-4257/

Table 1
Quantities to express water-related variables in foliage, where w_f (g) is the fresh leaf weight, w_d (g) is the leaf dry weight, A_{leaf} (m^2) is the one-sided leaf area and A_{ground} (m^2) is the ground covered area.

Variable	Abbreviation	Formula	Units
Foliar water content	FWC	$(w_f - w_d) / A_{leaf}$	g/cm^2
Canopy water content	CWC	$FWC * LAI$	g/cm^2
Fuel moisture content	FMC	$(w_f - w_d) / w_d$	–
Leaf area index	LAI	A_{leaf}/A_{ground}	m^2/m^2
Leaf mass per area	LMA	w_d/A_{leaf}	g/cm^2
Foliar biomass	FB	$LMA * LAI$	g/cm^2

Methods for retrieving these water-related biochemical properties of vegetation from remote sensing include empirical models in the form of a relationship with a particular vegetation index (VI) (Caccamo, Chisholm, Bradstock, Puotinen, & Pippen, 2012; Dennison, Roberts, Peterson, & Rechel, 2005; Garcia, Chuvieco, Nieto, & Aguado, 2008; Hunt, Li, Yilmaz, & Jackson, 2011; Peterson, Roberts, & Dennison, 2008; Sims & Gamon, 2003; Stow, Niphadkar, & Kaiser, 2005; Wang, Hunt, Qu, Hao, & Daughtry, 2011a; Wang, Hunt, Qu, Hao, & Daughtry, 2013), physically-based models that consider the full spectrum (Colombo et al., 2008; Riaño, Vaughan, Chuvieco, Zarco-Tejada, & Ustin, 2005; Romero, Aguado, & Yebra, 2012; Trombetti, Riaño, Rubio, Cheng, & Ustin, 2008; Vohland & Jarmer, 2008; Yebra & Chuvieco, 2009a; Zarco-Tejada, Rueda, & Ustin, 2003) and analytical methods that fit the spectrum solely in water bands using hyperspectral sensors (Cheng, Zarco-Tejada, Riaño, Rueda, & Ustin, 2006; Dennison et al., 2003; Roberts, Green, & Adams, 1997). Each one of these methodologies has its particular advantages and caveats, however the relative assessment of each method's performance has been neglected in literature, and validation using ground measurements has been limited (Jacquemoud et al., 2009).

Physically-based models retrieve water-related variables based on the inversion of radiative transfer modeling (RTM). The inversion using i) the minimization of a cost function that concurrently measures the discrepancies between the observed and predicted reflectance, through techniques such as iterative optimization (Zarco-Tejada et al., 2003) and look-up tables (LUTs) (Yebra & Chuvieco, 2009a); ii) artificial neural networks (ANNs) trained with a LUT of the RTM to predict the water-related variable from the observe reflectance (Trombetti et al., 2008); or iii) minimizing the discrepancies between the estimated variables and associated prior information with genetic algorithms (GAs) (Li, Cheng, Ustin, Hu, & Riaño, 2008).

RTM inversion has successfully been applied to the quantification and attribution of specific water-related biochemical variables of vegetation, such as FWC (Ceccato, Flasse, & Gregoire, 2002; Feret & Asner, 2011; Jacquemoud & Baret, 1990; Jacquemoud, Baret, Andrieu, Danson, & Jaggard, 1995; Kötz et al., 2004; Zarco-Tejada et al., 2003), CWC (Colombo et al., 2008; Kötz et al., 2004; Rubio, Riaño, Cheng, & Ustin, 2006; Trombetti et al., 2008), FMC (Colombo et al., 2008; Kötz et al., 2004; Riaño et al., 2005; Yebra & Chuvieco, 2009a), LAI (Atzberger, Darvishzadeh, Schlerf, & Le Maire, 2013; Darvishzadeh, Skidmore, Atzberger, & van Wieren, 2008; Fang & Liang, 2003; Gobron, Pinty, Verstraete, & Widlowski, 2000), LMA (Baret & Fourty, 1997; le Maire, Francois, & Dufrene, 2004; Riaño et al., 2005; Romero et al., 2012; Vohland & Jarmer, 2008) and FB (Kötz et al., 2004; Riaño et al., 2005). The major shortcoming of RTM methods is their parameterization, since they require many input variables to feed the model such as governing leaf and soil properties, and illumination and viewing angles of the scene. In particular, the simultaneous retrieval of water related biochemistry (e.g. FWC) and canopy structural parameters (LAI) is difficult firstly due to the relatively strong coupling between the quantity of leaf biochemical constituents (per unit leaf area) and vegetation amount/cover (structure) (Jacquemoud et al., 1995). Secondly, LMA retrievals through RTM inversion are hampered by the spectral similarity of soil and LMA (Ceccato, Flasse, Tarantola, Jacquemoud, & Gregoire, 2001; Ustin et al., 1998) and the fact that absorption features associated with LMA are obscured by liquid water in live leaves (Fourty & Baret, 1997).

On the other hand, VI (e.g. single ratio, normalized, combined) is a convenient tool to monitor water related biophysical and biochemical variables of the canopy and their temporal evolution. Based on the empirical relationship between water-related variables and reflectance at specific wavelengths, the main advantages of index-based methods are their fast processing and effectiveness. Those VIs in Tables 2 and 3 with bands in the visible (VIS) spectral region (400–700 nm) are indirectly related to water through correlations with leaf pigments (Chuvieco et al., 2004; Hardy & Burgan, 1999; Qi, Dennison, Spencer, & Riaño, 2012; Roberts, Dennison, Peterson, Sweeney, & Rechel, 2006; Stow, Niphadkar, & Kaiser, 2006, Stow et al., 2005; Yebra, Chuvieco, & Riano, 2008). Other VIs in Tables 2 and 3 based on near infrared (NIR, 700–1000 nm) and shortwave infrared (SWIR, 1000–2500 nm) bands have more direct relationships with water absorption (Ceccato, Gobron, Flasse, Pinty, & Tarantola, 2002; Cheng, Ustin, Riaño, & Vanderbilt, 2008; Cheng et al., 2013; Colombo et al., 2008; Dennison et al., 2005; Hunt et al., 2011; Wang et al., 2013; Yilmaz, Hunt, & Jackson, 2008; Yilmaz et al., 2008). LMA has been related to VI such as CAI, NDMI, DMCI, NDTI and LCA (Daughtry, Hunt, Doraiswamy, & McMurtrey, 2005; Nagler, Daughtry, & Goward, 2000; Romero et al., 2012; vanDeventer, Ward, Gowda, & Lyon, 1997; Wang, Hunt, Qu, Hao, & Daughtry, 2011b; Wang et al., 2011a). Recently, parametric models have been used to assess the performance of standard VI (Danson & Bowyer, 2004; Wang et al., 2011a) and to create new indexes dedicated to CWC (Ceccato, Gobron, Flasse, Pinty, & Tarantola, 2002), FWC (Feret et al., 2011) and LMA (Feret et al., 2011; le Maire et al., 2004; Romero et al., 2012). However, the performance of these new indexes against ground data and their comparison with alternative methods are scarce (Jacquemoud et al., 2009; Wang et al., 2013).

Finally, curve-fitting techniques can retrieve CWC from Advanced Visible Infrared Imaging Spectrometer (AVIRIS) data (Dennison et al., 2003, 2005; Green, Conel, & Roberts, 1993; Roberts et al., 1997, 2006). These methods fit image spectra with the absorption spectra of liquid water scaled by a path length. Various studies have validated their proposed methodologies in relation to this physically based CWC assuming its superiority (Cheng et al., 2008; Trombetti et al., 2008). Nevertheless, studies that quantitatively assess the relation between spectrally fitted CWC against actual in-situ field measurements are uncommon (Champagne, Staenz, Bannari, McNairn, & Deguise, 2003; Cheng et al., 2008).

The main goal of this study is the assessment of a wide range of methods using the optical domain of the spectra to retrieve biophysical and biochemical parameters related to water in vegetation (FWC, CWC, and FMC) and several interrelated variables (LAI, LMA, and FB). Methods are applied to hyperspectral AVIRIS data and this AVIRIS data convolved to Moderate Resolution Imaging Spectrometer (MODIS)-like data, within a multitemporal frame and stratified by cover type (i.e. grasses, shrubs and forest). Methods tested are curve-fitting techniques using AVIRIS data, standard and recently designed VI, best band combination indexes and AVIRIS PROSAIL and MODIS CWC PROSAIL inversion.

2. Materials and methods

2.1. Study site

In-situ FWC, CWC, FMC, LAI, LMA and FB measurements of vegetation were made at Stanford University's Jasper Ridge Biological Preserve (JRBP) located in the central region of the Coast Range of California, USA (Fig. 1). JRBP protects a Mediterranean-type ecosystem at an approximate elevation of 150 m above sea level. The Preserve's Mediterranean climate is characterized by a total annual average precipitation of 654 mm, mainly falling during the cool wet season from November to

Table 2
Spectral indexes calculated for AVIRIS including their shortened acronym, mathematical formulation and reference.

Index	Acronym	Formula	Reference
Normalized Difference Vegetation Index	NDVI	$(\rho_{850} - \rho_{670}) / (\rho_{850} + \rho_{670})$	Tucker (1979)
Modified Normalized Difference Vegetation Index	mNDVI	$(\rho_{750} - \rho_{705}) / (\rho_{750} + \rho_{705})$	Gitelson Kaufman, and Merzlyak (1996)
Enhanced Vegetation Index	EVI	$2.5\ (\rho_{858.5} - \rho_{645}) / (\rho_{858.5} + 6\rho_{645} - 7.5\rho_{469} + 1)$	Huete et al. (2002)
Normalized Difference Water Index	NDWI	$(\rho_{858.5} - \rho_{1240}) / (\rho_{858.5} + \rho_{1240})$	Gao (1996)
Short Infrared Water Stress Index	SIWSI	$(\rho_{858.5} - \rho_{1640}) / (\rho_{858.5} + \rho_{1640})$	Fensholt and Sandholt (2003)
Moisture Stress Index	MSI	ρ_{1599}/ρ_{819}	Hunt and Rock (1989)
Water Index	WI	ρ_{900}/ρ_{970}	Penuelas, Pinol, Ogaya, and Filella (1997)
Cellulose Absorption Index	CAI	$0.5\ (\rho_{2000} + \rho_{2200}) - \rho_{2100}$	Nagler et al. (2000)
Normalized Difference Infrared Index	NDII	$(\rho_{850} - \rho_{1600}) / (\rho_{850} + \rho_{1600})$	Hardisky, Klemas, and Smart (1983)
Normalized Dry Matter Index	NDMI	$(\rho_{1649} - \rho_{1722}) / (\rho_{1649} + \rho_{1722})$	Wang et al. (2011a)
Simple Ratio Water Index	SRWI	ρ_{860}/ρ_{1240}	Zarco-Tejada et al. (2003)
Reciprocal of Moisture Stress Index	RMSI	ρ_{860}/ρ_{1650}	Hunt and Rock (1989)
NDII/NDMI	NDII/NDMI	See formulas above	Wang and Li (2012)
NDWI/NDMI	NDWI/NDMI	See formulas above	Wang and Li (2012)
MSI/NDMI	MSI/NDMI	See formulas above	Wang and Li (2012)
RMSI/NDMI	RMSI/NDMI	See formulas above	Wang and Li (2012)
SRWI/NDMI	SRWI/NDMI	See formulas above	Wang and Li (2012)
Dry Matter Content Index	DMCI	$(\rho_{2305} - \rho_{1495}) / (\rho_{2305} + \rho_{1495})$	Romero et al. (2012)
Normalized Difference LMA 1340 nm, 1710 nm	$ND_{1340–1710}$	$(\rho_{1340} - \rho_{1710}) / (\rho_{1340} + \rho_{1710})$	le Maire et al. (2008)
Normalized Difference Tillage Index	NDTI	$(\rho_{1650} - \rho_{2215}) / (\rho_{1650} + \rho_{2215})$	vanDeventer et al. (1997)
Lignin–Cellulose Absorption Index	LCA	$2\rho_{2205} - (\rho_{2165} + \rho_{2330})$	Daughtry et al. (2005)
Ratio Index FWC 1062 nm, 1393 nm	$RI_{1062–1393}$	ρ_{1062}/ρ_{1363}	Feret et al. (2011)
Normalized Difference FWC 1062 nm, 1393 nm	$ND_{1062–1393}$	$(\rho_{1062} - \rho_{1393}) / (\rho_{1062} + \rho_{1363})$	Feret et al. (2011)
Ratio Index LMA 1368 nm, 1722 nm	$RI_{1368–1722}$	ρ_{1368}/ρ_{1722}	Feret et al. (2011)
Normalized Difference LMA 1368 nm, 1722 nm	$ND_{1368–1722}$	$(\rho_{1368} - \rho_{1722}) / (\rho_{1368} + \rho_{1722})$	Feret et al. (2011)

April (Ackerly, 2004; Ackerly, Knight, Weiss, Barton, & Starmer, 2002). A seasonal drought extends from May to September, with less than 50 mm precipitation/month throughout most of the growing season. The site covers a wide range of vegetation physiognomic types dominated by woody plant communities including chaparral and woodlands. Non-woodland communities include the California annual and perennial grasses and wetlands (Porter & Corelli, 2002). These communities have significantly different phenological characteristics that produce major functional differences in terms of canopy development, energy balance, gas exchange properties, and nutrient use patterns (Ustin, Duan, Hart, & Haxo, 1994). For instance, chaparral is dominated by evergreen shrub species with small, thick, sclerophyllous leaves (Mooney & Dunn, 1970). Topographically driven soil moisture availability, with drier soils on higher elevation and south-facing slopes, is the most important environmental factor underlying these vegetation communities (Ackerly et al., 2002; Cornwell, Schwilk, & Ackerly, 2006). Geologically, this site is part of the Central Coast Range, in the Franciscan Complex, an Early Cretaceous accretionary mélange containing blocks of chert, greywacke, greenstone, blue schist and serpentinized ophiolite. The main soils are Alluvial, Tertiary sandstone and Franciscan complex (Greenstone and Serpentine) (Coleman, 2004; Oze, Skinner, Schroth, & Coleman, 2008) (Fig. 1).

2.2. Field data collection and water-related variables estimation

Field measurements were made at 39 sampling sites (Fig. 1) stratified into 13 sites per cover type, distinguishing between grass (g), shrub (s) and forest (f) types on three different dates: May 12th and September 21st, 2006 and August 14th, 2007. Within a cover type, each site might contain a different mix of species. Grasslands are dominated by annuals, both grasses and forbs, and perennial grasses. Table 4 summarizes woody plant species encountered in each shrub and forest sampling site.

Field sampling protocols varied by cover type. In grasslands, three sample sizes were collected: i) a small size envelope (SE) with at least 10 leaves for calculating the water/dry mass relation to leaf area; ii) three big envelops (BE) of at least 100 g leaf samples, without roots, to estimate the water to dry mass spatial variability of the plot and iii) a big bag (BB) with all leaves on a 50 by 50 cm sub-plot within the 10 by 10 m sample plot to find the leaf area to ground area relationship (LAI). Shrub and forest sites were measured with: i) SE leaf samples and ii) BE with the terminal shoots (shrubs) and leaves (forest) of each dominant species. Both samples were collected for the same purpose as the grasses, but LAI was measured indirectly using hemispherical photographs. Four of them were taken for each plot in cardinal directions under diffuse light conditions (at dawn or dusk) for forests and

Table 3
Spectral indexes calculated for MODIS-like data including their shortened acronym, mathematical formulation and reference. MODIS band wavelengths: ρ_1 (645 nm), ρ_2 (859 nm), ρ_3 (469 nm), ρ_4 (555 nm), ρ_5 (1240 nm), ρ_6 (1640 nm), and ρ_7 (2130 nm).

Index	Acronym	Formula	Reference
Normalized Difference Vegetation Index	NDVI	$(\rho_2 - \rho_1) / (\rho_2 + \rho_1)$	Rouse, Haas, Schell, and Deering (1973)
Normalized Difference Water Index	NDWI	$(\rho_2 - \rho_5) / (\rho_2 + \rho_5)$	Gao (1996)
Normalized Difference Infrared Index	NDII	$(\rho_2 - \rho_6) / (\rho_2 + \rho_6)$	Hardisky et al. (1983)
Normalized Difference Water Index (b 7)	NDW7	$(\rho_2 - \rho_7) / (\rho_2 + \rho_7)$	Rouse et al. (1973)
Enhanced Vegetation Index	EVI	$2.5\ (\rho_2 - \rho_1) / (\rho_2 + 6\rho_1 - 7.5\rho_3 + 1)$	Huete et al. (2002)
Soil Adjusted Vegetation Index	SAVI	$(1 + 0.5)\ (\rho_2 - \rho_1) / (\rho_2 + \rho_1 + 0.05)$	Huete (1988)
Global Environmental Monitoring Index	GEMI	$\eta\ (1 - 0.25\eta) - [\rho_1 - 0.125 / (1 - \rho_1)];\ \eta = 2$ $(\rho_2^2 - \rho_1^2) + 1.5\rho_2 + 0.5\rho_2 / (\rho_2 + \rho_1 + 0.5)$	Pinty and Verstraete (1992)
Visible Atmospherically Resistant Index	VARI	$(\rho_4 - \rho_1) / (\rho_4 + \rho_1 - \rho_3)$	Gitelson, Kaufman, Stark, and Rundquist (2002)
Global Vegetation Moisture Index	GVMI	$(\rho_2 + 0.1) - (\rho_6 + 0.02) / (\rho_2 + 0.1) + (\rho_6 + 0.02)$	Ceccato, Gobron, Flasse, Pinty, and Tarantola (2002)

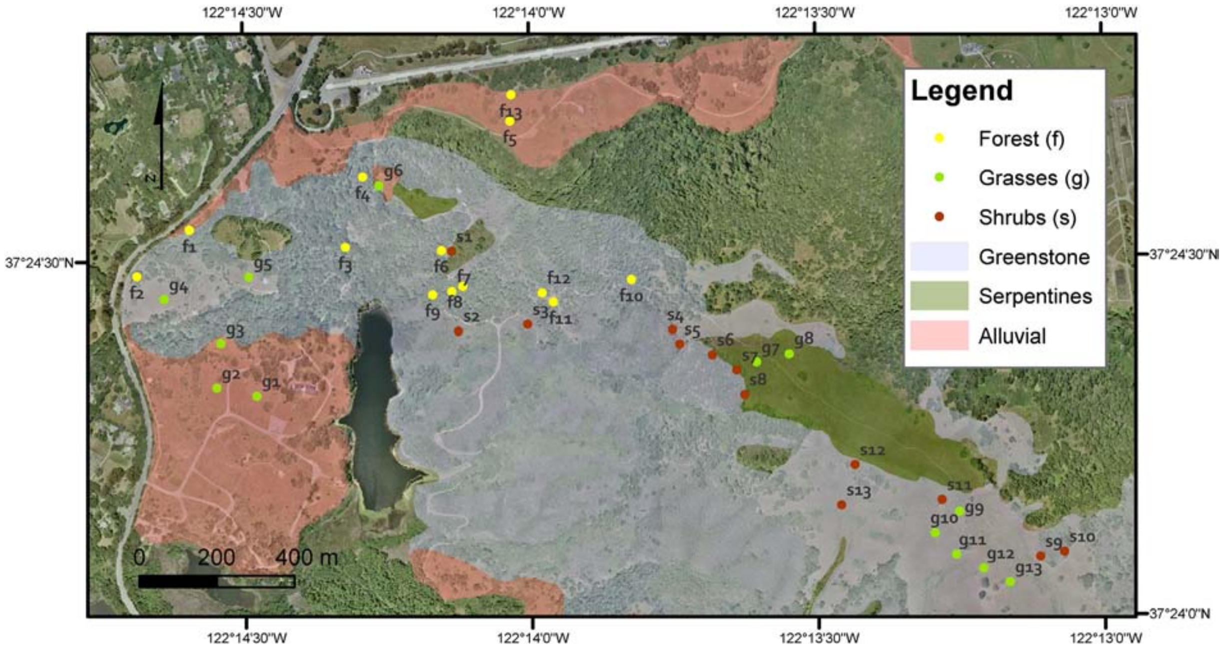

Fig. 1. Orthophoto of the Jasper Ridge Biological Preserve with a soil map (after Coleman, 2004) and the location of the sampling points for each cover type.

shrubs at a height of 0.7 m and 0.2 m, and 2.5 m and 1 m away from the center of the plot, respectively. LAI was estimated with HemiView canopy analysis software (Delta-T Devices Ltd., Cambridge, UK). For each sample site and container, fresh weight and oven dry weight (at 54 °C for at least 48 h) were calculated using gravimetric methods. Leaf area was calculated from visual delineation of digital photographs taken of the fresh SE leaf samples.

For each cover type, the six variables were calculated according to their definitions (Table 1). In addition, FWC was also computed by multiplication of FMC by LMA. To circumvent sampling data set size limitations, averaging strategies were explored. LMA and LAI values were derived using an average of the three dates (LMA^{date} and LAI^{date}, respectively). LMA was also averaged solely by species ($LMA^{species}$) or by species and dates simultaneously ($LMA^{species\&date}$). In the case of the grasses, an average per soil type was also investigated (LMA^{soil}). Finally, the use of an annual average of LMA per species was explored using data from literature (LMA^{biblio}) from our study site (Ackerly et al., 2002). These approaches take advantage of the fact that FMC is leaf/ground area independent, assumes that LMA is species dependent (Shipley & Vu, 2002) and remains relatively constant throughout the year (Ackerly et al., 2002), although small overall declines have been reported during the drought period (Garnier et al., 2001) and accumulation during favorable periods of carbon gain (Ustin et al., 2012).

2.3. Remote sensing data and preprocessing

AVIRIS data were collected over JRBP on May 14th and September 22nd, 2006 and August 13th, 2007. There was at most a two-day mismatch between field sampling and AVIRIS acquisition within which weather remained stable. Vegetation regulates its water content through evapotranspiration and root uptake (Jackson, Sperry, & Dawson, 2000); therefore it is expected little impact of this mismatch, especially in the context of the estimation of seasonal vegetation water content variations. AVIRIS is an airborne imaging spectrometer that collects spectra with a nominal 10 nm full width half maximum, over 224 spectral bands between 380 and 2500 nm and a spatial resolution ranging from 3 m to 20 m depending on the platform and acquisition altitude. In order to capture the entire study area, two AVIRIS E–W overlapping flight lines with 3.3 m spatial resolution were necessary for May 2006 and August 2007, whereas one single flight line with 20 m resolution was flown in September 2006. All images were radiometrically calibrated by Jet Propulsion Laboratory (JPL) and co-registered using a high spatial resolution orthophoto (15 cm). AVIRIS at-sensor radiance data were normalized to nadir-view applying an empirical BRDF correction with ATCOR-4 version 6.3 (Richter & Schläpfer, 2013). Water vapor was estimated directly from the 940/1140 nm features in the radiance data. After eliminating noisy atmospheric absorption bands from the 1350 to 1450 nm and from the 1850 to 1950 nm regions, spectral

Table 4
List of woody plant species encountered in each shrub (s) and forest (f) sampling site.

Species	Common name	Site
Lepechinia calycina (Benth.) Epling ex Munz	Woodbalm	s01
Ceanothus cuneatus (Hook.) Nutt.	Buckbrush	s01, s03
Baccharis pilularis DC.	Coyotebrush	s01, s11, s12, s13
Adenostoma fasciculatum Hook & Arn.	Chamise	s02, s03, s04, s05, s06, s07, s08, s10
Eriodictyon californicum (Hook. & Arn.) Torr.	California yerba santa	s05
Quercus douglasii Hook. & Arn.	Blue oak	s06, s07, f10, f11, f12, f13
Heteromeles arbutifolia (Lindl.) M. Roem.	Toyon	s07
Artemisia californica Less.	Coastal sagebrush	s09, s10
Mimulus aurantiacus W. Curtis	Orange bush monkey flower	s10
Quercus agrifolia Née	California live oak	f01, f02, f03, f04, f05, f06, f07, f08, f09, f12
Quercus lobata Née	Valley oak	f03, 05 and f13

response at the sensor was generated for the 218 remaining bands using the standard temperate atmosphere look-up type. Normalization between flight lines was accomplished simultaneously to the conversion to apparent surface reflectance using ATCOR. Firstly, the May 2006 west (W) flight line was calibrated with in-situ field spectra simultaneously to run ATCOR-4; then the May 2006 east (E) flight line was cross calibrated with W using overlapping targets and the same targets between E and W flight lines in August 2007, and finally homogeneous spectral invariant targets, e.g. basalts in the southeast area of JRBP and roofs, soils and asphalt, were chosen to normalize between the three dates. AVIRIS spectra of each plot were then extracted and spectrally degraded to the MODIS spectral response function by convolving corresponding AVIRIS bands using a Gaussian function fit to band centers and the Full-Width-Half-Maximum (FWHM) reflectance, keeping its AVIRIS original spatial resolution. A total of 117 AVIRIS spectra, and their transformed MODIS-like spectra, were extracted, since there were thirteen plots for each of the three land cover types and measured three dates for each one.

2.4. Evaluation of methods to estimate water-related variables from remote sensing data

Several methods were applied to retrieve plant water-related variables: FWC, CWC, FMC, LAI, LMA and FB from AVIRIS and MODIS-like spectra. The root mean square error (RMSE) and a relative RMSE (rRMSE), calculated as RMSE divided by the mean of the variable as measured in the field, evaluated the performance of the methods, following Richter, Atzberger, Hank, and Mauser (2012). rRMSE allows comparison between variables of different ranges, since it is insensitive to magnitude of values and less sensitive to outliers (Richter et al., 2012).

2.4.1. Retrievals from AVIRIS

Four families of methods were applied to AVIRIS data: two curve-fitting techniques, a variety of standard VI, a set of best band combination indexes and PROSAIL inversion. Each method is described in detail below.

2.4.1.1. Curve-fitting techniques. The first curve-fitting method assessed uses a moderate spectral resolution atmospheric transmittance algorithm (MODTRAN) spectral fitting technique based on water absorption coefficients defined by Curcio and Petty (1951) who derived the equivalent liquid water depth. The method simultaneously fits water vapor and liquid water estimates for improved atmospheric calibrations. The different phases of water have absorption maxima about 40 nm apart, located between 925 and 1050 nm. The MODTRAN algorithm is implemented in Atmospheric Correction Now (ACORN) software (Imaging & Geophysics, 2002), in mode 1.5. The ACORN-fitting method uses bands centered around 940 nm, 1140 nm, or both. The retrieved measure is the equivalent depth of water over the area of a pixel that is required to fit the water absorption model in the atmospheric calibration procedure. These methods will be referred as ACORN CWC 940 nm, ACORN CWC 1140 nm and ACORN CWC 940 & 1140 nm, depending on the bands used. For the second method, non-linear least squares fitted the absorption spectrum of liquid water to the vegetation reflectance spectra. Reflectance spectra were modeled from 850 nm to 1100 nm, a spectral region spanning a liquid water absorption maximum at 970 nm. Background reflectance was assumed to have a linear trend across this spectral region. The CWC model used by Gao and Goetzt (1995), Roberts et al. (1997), and Dennison et al. (2003) was applied to each reflectance spectrum:

$$\rho_\lambda = (a + b\lambda)e^{-t\alpha_\lambda} \tag{1}$$

where ρ is reflectance at wavelength λ, a is the intercept term for the background reflectance trend, b is the slope term for the background reflectance trend, α_λ is the absorption coefficient of liquid water at wavelength λ, and t is the canopy EWT. We refer to this method as CWC 970 nm.

2.4.1.2. Standard VI. AVIRIS was used to calculate a wide range of published standard greenness and water absorption-based VI previously identified to be good predictors of water and dry mass in the literature (Table 2).

2.4.1.3. Best band combination indexes. Field measured values help identify an optimal combination of spectral bands in the shape of a given type of index for each variable (Feret et al., 2011; le Maire et al., 2004; Wang et al., 2011b). Normalized difference indexes ($ND_{xy} = (\rho_{\lambda x} - \rho_{\lambda y}) / (\rho_{\lambda x} + \rho_{\lambda y})$) were calculated using all possible AVIRIS band combination. We only present the indexes that provided the minimum RMSE between calculated and water related variables sampled on the ground for all the plots. The main goal of applying this method is to understand which band combinations better relate to each water variable per cover type.

2.4.1.4. PROSAIL. Radiative transfer modeling (RTM) inversion was applied linking the PROSPECT leaf model (Jacquemoud et al., 2009) with SAIL canopy reflectance model, after including a correction for the hotspot effect (Verhoef, 1984; Kuusk, 1985; Verhoef, 1985). In PROSPECT, leaf single scattering albedo is calculated as a function of the leaf cell–air interface refractive index (n), the number of layers (N) and the absorption coefficients related to the concentration (units of mass per unit leaf area) of certain biochemical constituents (Jacquemoud, Bacour, Poilve, & Frangi, 2000). For PROSPECT-5, these constituents are Chlorophyll a + b, carotenoid content, FWC, and LMA (Table 5). Scaling up relationships linking the leaf to canopy level, PROSPECT-5 is connected with SAIL, a 1D turbid medium radiative transfer model, that requires as inputs: LAI; leaf angle distribution (LAD); viewing geometry: solar zenith, observer's zenith and azimuth; soil reflectance; and hotspot parameter as implemented by Kuusk (1991) and defined as the ratio between the average size of the leaves and the canopy height (Verhoef, 1985). The range of biochemical/structural variables selected to model the spectral responses were set to comprise the range of actual values according to the cover type (Table 5). The measurement geometry and the zenith solar angle were extracted from the AVIRIS image metadata for each pixel. The fraction of diffuse incoming solar radiation *skyl* was assigned a fixed value across all wavelengths of 0.1 as in similar studies (Cho, Skidmore, Corsi, van Wieren, & Sobhan, 2007; Schlerf & Atzberger, 2006). A soil brightness parameter (p) accounted for changes induced by moisture and roughness in soil brightness. Since Chlorophyll a + b, and carotenoid content do not have a strong impact upon FWC and LMA estimations (Ceccato et al., 2001), they were fixed at 50 $\mu g/cm^2$ and 10 $\mu g/cm^2$, respectively. The *hotspot* parameter was set in agreement with the literature: for grasses 0.5, for shrubs 0.01, and for forests 0.05 (Verhoef & Bach, 2007). In addition, the use of ancillary data to retrieve FWC, LMA and LAI was explored in two more scenarios. A first one incorporated known values of LAI derived from field data and a second one included spectra from bare soil obtained from the image for each soil type. The soil type was identified using a soil map of the site provided by JRBR and based on Coleman (2004) and the spectrum of each soil class was taken from a pure bare soil pixel of the corresponding class, as close as possible to the sampling site. Following Riaño et al. (2005) who showed that higher FWC hides the LMA absorptions in the spectra, FMC was also calculated using LMA from the drier samples, selected using a threshold in FMC <75%, to replace LMA from wetter samples, assuming LMA is time invariant throughout the year. To find the optimal spectra corresponding to a given measurement, a merit function was calculated between measured and simulated spectra. The model selects by exhaustive iteration the set of parameters that minimize the merit function

Table 5
Specific ranges for the nine input parameters to invert the PROSAIL model.

Parameter	Units	Grasses		Shrubs		Forests	
		Range	Step	Range	Step	Range	Step
Leaf structure (N)	–	1.5–1.9	0.2	1.5–1.9	0.2	1.5–1.9	0.2
Leaf chlorophyll (Cab)	μg/cm^2	50		50		50	
Leaf carotenoid (Car)	μg/cm^2	10		10		10	
Foliar water content (FWC)	g/cm^2	0–0.03	0.001	0.001–0.03	0.001	0.005–0.025	0.001
Leaf mass per area (LMA)	g/cm^2	0.006–0.03	0.001	0.005–0.04	0.001	0.01–0.02	0.001
Average leaf angle (angl)	°	50		50–90	20	10–50	20
Leaf area index (LAI)	m^2/m^2	0.1–2	0.1	0.1–2.5	0.1	1–2.5	0.1
Hot spot size (hspot)	–	0.5		0.01		0.05	
Diffuse/direct rad. (skyl)	–	0.1		0.1		0.1	

Δ^2 (Zarco-Tejada et al., 2003) given by the following equation: $\Delta^2 = \Sigma\,(\rho_m(\lambda_i) - \rho(\lambda_i, P))^2$ where $\rho_m(\lambda_i)$ is the measured canopy spectral reflectance and $\rho(\lambda_i, P)$ is the modeled canopy spectral reflectance with a set of P parameters. All the bands were used to compute the error between estimated and measured reflectance (Jacquemoud, 1993).

2.4.2. Retrievals from MODIS-like data

2.4.2.1. Standard VI. Nine standard VIs in Table 3 identified from the literature to be good predictors of water-related properties of vegetation were calculated for the MODIS-like spectra.

2.4.2.2. Best band combination index. Finally, we searched for optimal combinations of spectral MODIS-like bands in the shape of different types of indexes that predict each variable using ground measured values and linear regression. Index types selected were: i) ratios (RI_{xy}: $\rho_{\lambda x}/\rho_{\lambda y}$); ii) normalized differences ($ND_{xy} = \rho_{\lambda x} - \rho_{\lambda y} / \rho_{\lambda x} + \rho_{\lambda y}$); iii) three bands ($3BI_{xyz} = \rho_{\lambda x} / (\rho_{\lambda y} + \rho_{\lambda z})$); and iv) first derivatives of bands (D_{xy}), that due to the discrete characteristic of the spectral sampling intervals was approximated by the finite difference as: $D_{xy} = (\rho_{\lambda x} - \rho_{\lambda y}) / (\lambda_x - \lambda_y)$. A total of 200 indexes were calculated from MODIS-like bands. The indexes were generated for every combination of bands and, similarly to the AVIRIS case, the index for each variable was selected using the criterion of minimum RMSE between calculated and water related variable sampled in the ground for all the plots.

2.4.2.3. PROSAIL inversion. An inversion of the linked radiative transfer model PROSAIL, through an artificial neural network (ANN) was applied to MODIS-like data. The model was designed by Trombetti et al. (2008) to generate monthly CWC maps from MODIS data for the continental U.S., which showed realistic changes in water contents given climate patterns and phenological timing. The PROSAIL model was specifically designed for homogeneous canopies such as grasses but Trombetti et al. (2008) applied different equations for grass, shrub and forest canopies based on the model calibration with CWC AVIRIS estimates. We applied this model to assess its behavior in relation to CWC for the three cover types.

3. Results

Table 6 summarizes the method selected based on the lowest RMSE to estimate each variable from field data per cover type. FWC and CWC are estimated through their relation to FMC by LMA annual average obtained from bibliographic sources (LMA^{biblio}) in the case of shrubs and forests. For grasses, LMA averaged by date (LMA^{date}) is used to estimate LAI whereas LMA is estimated as the averaged value by date and soil. Fig. 2 shows the box plot for each measured variable.

3.1. Curve-fitting methods

Curve-fitting techniques were tested for the retrieval of CWC. ACORN CWC 940 nm failed to render reliable results with most values being zero. ACORN failed to provide liquid water estimations in the August 2007 E flight line, where some grass and shrub sites were located. Hence, ACORN CWC 940 nm, ACORN CWC 1140 nm and ACORN CWC 940 & 1140 nm were evaluated for 31 out of the 39 grass sites and 26 out of the 36 shrub sites. All 39 forest sites could be retrieved as they were located in the W flight line. Fig. 3 shows the relationships of CWC with the three curve-fitting techniques in the case of forests. The three methods show very large RMSE compared with the rest of the methods (Table 7). Out of the three methods, better results were achieved using ACORN CWC 940 & 1140 nm and CWC 970 nm. CWC 970 nm overestimates grasses by ~ three times whereas shrubs had the same magnitude. In forests, ACORN 940 & 1140 nm and CWC 970 nm overestimated CWC by ~ seven and five times respectively. Considering the three cover types, using the CWC 970 nm feature (Table 7), CWC from forests was the least accurate, with grasses and shrubs overestimated by two times.

3.2. Standard VI

Table 7 shows the RMSE of the best retrieval per variable using AVIRIS standard VI. Meanwhile, Fig. 4 presents the rRMSE obtained between the six variables and the standard VI with the best performances per variable. It is clear from our results that the best retrievals of FWC, CWC and FMC for grasses and shrubs are provided by greenness VI such as NDVI, mNDVI, EVI and WI (Fig. 4). For grasses, NDVI provides the best CWC and FMC, whereas EVI or WI retrieves better FWC. In

Table 6
Water-related variable calculation from field data in big bags (BBs) or big envelopes (BEs) averaged by the three dates (date), date and soil (date&soil) or annual average obtained from bibliographic sources (biblio).

Variable	Units	Grasses	Shrubs	Forests
FWC	g/cm^2	$FMC_{BB} * LMA^{soil}$	$FMC_{BE} * LMA^{biblio}$	$FMC_{BE} * LMA^{biblio}$
CWC	g/cm^2	CWC_{BB}	$FMC_{BE} * LMA^{biblio} * LAI$	$FMC_{BE} * LMA^{biblio} * LAI$
FMC	–	FMC_{BB}	FMC_{BE}	FMC_{BE}
LAI	m^2/m^2	$W_{d,BB} / (A * LMA^{date})$	LAI	LAI
LMA	g/cm^2	$LMA^{date\ \&soil}$	LMA^{biblio}	LMA^{biblio}
FB	g/cm^2	$LMA * LAI_{BB}$	$LMA^{biblio} * LAI$	$LMA^{biblio} * LAI$

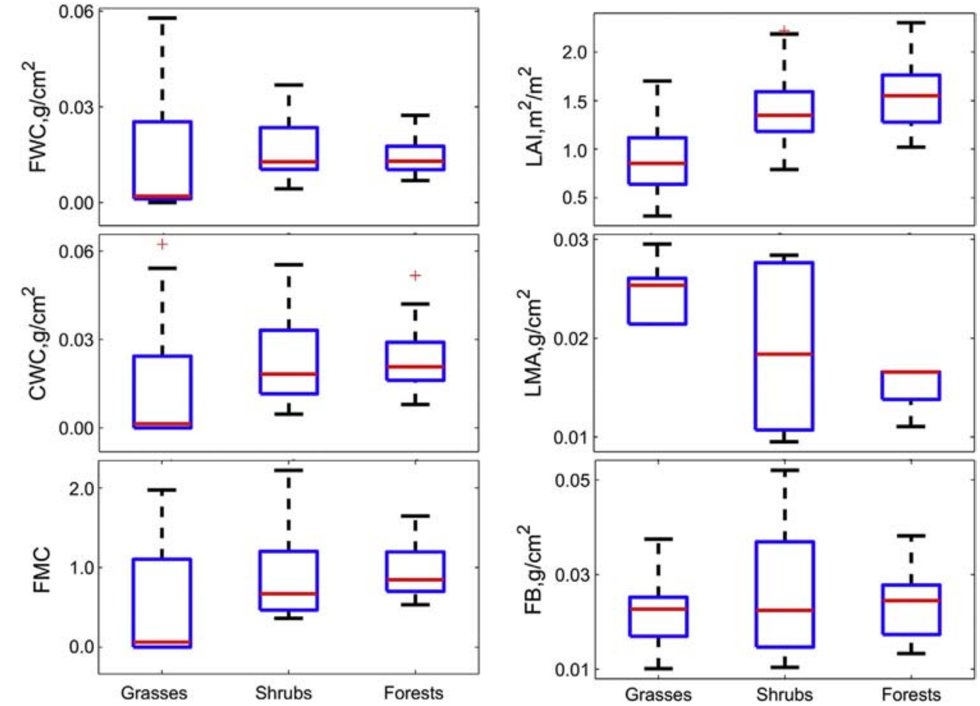

Fig. 2. Box plots of the ground-measured values for each water-related variable for each cover type.

the case of shrubs, WI is the best index for FWC and CWC, whereas mNDVI obtains better FMC. In the case of forests, NDVI is still effective but RI1062/1393 and WI outperform it to derive CWC and FMC, respectively. The recently designed ND1340/1710 and RI1368/1722 retrieve well LAI on grasses and RMSI does on shrubs with similar results from SIWSI and NDII. MSI/NDMI provides the best retrievals of LAI for forests with similar performances from NDMI, NDII and SIWSI. For LMA, all the seven standard VIs selected give similar performances, with better results using MSI/NDMI for grasses, LCA for shrubs and NDMI for forests. ND1368/1722 retrieves better FB for grasses and shrubs whereas MSI/NDMI is the best index for forests. Considering all the variables, forests are always better retrieved except for the case of LMA for grasses, where standard VI gives the best results. Considering the three cover types together, NDVI retrieves better FWC, CWC and FMC than other different indexes with 73, 61 and 57% rRMSE, respectively (Fig. 4 and Table 7). NDWI/NDMI estimates better LAI and LMA with a rRMSE of 23 and 27%, respectively. For LMA, the error for shrubs is much larger than the one obtained for grasses and forests. RMSI/NDMI predicts FB better with a 37% rRMSE. Only for LAI, the rRMSE using NDWI/NDMI is the same than segregating per cover type.

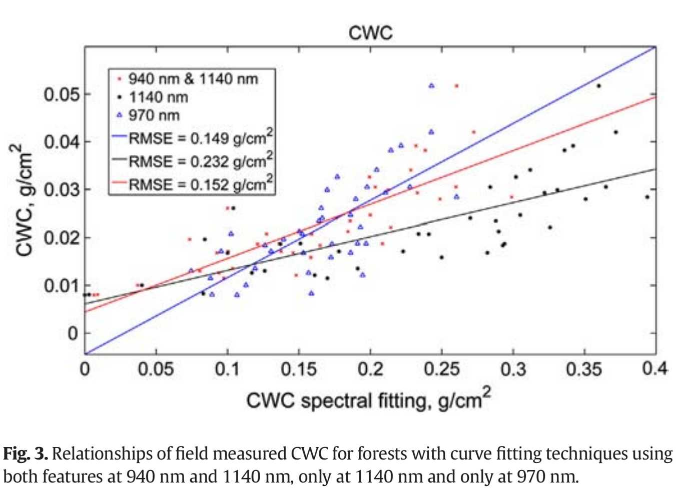

Fig. 3. Relationships of field measured CWC for forests with curve fitting techniques using both features at 940 nm and 1140 nm, only at 1140 nm and only at 970 nm.

Fig. 5 presents the performance of the nine selected VIs from MODIS-like spectra for each variable. Out of all the indexes, VARI is the most effective index for estimating FWC, CWC and FMC for grasses and shrubs (Table 7). NDVI for grasses and SAVI and EVI for shrubs also provides good results. In forests, VARI works well for FWC, but EVI outperforms it for FMC, whereas NDWI was the most effective together with NDII to retrieve CWC. NDW7 retrieves LAI well for the three cover types with NDII working also well for shrubs and forests. LMA and FB are well retrieved by GVMI. The index also works well for LAI in the case of forests and shrubs.

3.3. Best band combination indexes

Fig. 7 shows that FWC, CWC and FMC out of the six variables benefited most from using an AVIRIS best band combination index with bands in the longer wavelength SWIR (Table 7). FMC is the variable that improves the most reducing the rRMSE to 10% for grasses, 21% for shrubs and 9% for forests, using $ND_{2045–2165}$, $ND_{2080–2160}$ and $ND_{2285–2434}$ instead of NDVI, mNDVI and WI respectively. Fig. 4 shows that FWC and CWC in grasses also improve 10% and 9%, using in both cases $ND_{2325–2434}$ in relation to the results obtained with NDVI. LAI and LMA or FB slightly improves from the use of standard VI, and only FB improves 3% in rRMSE for forests when using $ND_{2175–2315}$ in relation to MSI/NDMI.

For MODIS-like data, no best band combination index outperforms VARI to retrieve FWC, CWC and FMC, except in the case of shrubs where SWIR (ρ_6, $\rho_{3\text{ and }}\rho_7$) improves FMC retrieval to 5% (Table 7). Interestingly, this band combination also provides the best retrievals of LMA to 4% in relation to the use of band 4 instead of 3 and improves to 3% the retrievals of FB in relation to GVMI.

3.4. PROSAIL

Using RTM inversion over AVIRIS data, biochemistry variables are best retrieved for forest and worst for grasses (Fig. 6 and Table 7). Incorporating a known soil spectrum improves FMC retrievals for the three cover types reducing rRMSE to 16, 29 and 8% for grasses, shrubs and

Table 7
RMSE obtained for water-related variables by cover type from AVIRIS and MODIS-like data using different methodologies.

	Var	AVIRIS							MODIS			
		Standard VI		Best band index		PROSAIL	970 nm	PROSAIL	Standard VI		Best band index	
Grasses	FWC	NDVI	0.007	$ND_{2325–2434}$	0.006	0.019	–	–	NDVI	0.007	$\rho_1 / (\rho_2 + \rho_7)$	0.007
	CWC	NDVI	0.006	$ND_{2325–2434}$	0.005	0.019	0.046	0.037	VARI	0.007	$\rho_1 / (\rho_2 + \rho_7)$	0.007
	FMC	NDVI	0.265	$ND_{2045–2165}$	0.216	0.524	–	–	VARI	0.265	$\rho_1 / (\rho_2 + \rho_7)$	0.273
	LAI	$ND_{1340–1710}$	0.255	$ND_{1662–1752}$	0.258	0.454	–	–	NDW7	0.280	$\rho_5 / (\rho_3 + \rho_7)$	0.273
	LMA	MSI/NDMI	0.002	$ND_{1662–1732}$	0.002	0.016	–	–	GEMI	0.002	$(\rho_3 - \rho_5) / (0.47 - 1.24)$	0.002
	FB	$RI_{1062–1393}$	0.006	$ND_{1168–1206}$	0.005	0.017	–	–	GVMI	0.006	$(\rho_2 - \rho_6) / (0.86 - 1.63)$	0.006
Shrubs	FWC	mNDVI	0.006	$ND_{2080–2160}$	0.005	0.012	–	–	VARI	0.006	$\rho_6 / (\rho_3 + \rho_7)$	0.006
	CWC	WI	0.008	$ND_{1550–1630}$	0.007	0.018	0.041	0.067	VARI	0.008	$\rho_4 / (\rho_1 + \rho_3)$	0.008
	FMC	mNDVI	0.412	$ND_{2080–2160}$	0.212	0.912	–	–	VARI	0.413	$\rho_6 / (\rho_3 + \rho_7)$	0.363
	LAI	RMSI	0.224	$ND_{928–947}$	0.208	0.523	–	–	NDII	0.226	$\rho_4 / (\rho_1 + \rho_6)$	0.215
	LMA	LCA	0.007	$ND_{1550–1750}$	0.006	0.013	–	–	GVMI	0.007	$\rho_6 / (\rho_3 + \rho_7)$	0.007
	FB	$RI_{1062–1393}$	0.009	$ND_{2100–2160}$	0.009	0.019	–	–	GVMI	0.010	$\rho_6 / (\rho_4 + \rho_7)$	0.010
Forests	FWC	$RI_{1062–1393}$	0.003	$ND_{2265–2134}$	0.002	0.009	–	–	VARI	0.003	$(\rho_2 - \rho_6) / (0.86 - 1.63)$	0.003
	CWC	$RI_{1062–1393}$	0.006	$ND_{2475–2394}$	0.006	0.012	0.149	0.181	NDWI	0.007	$\rho_2 / (\rho_5 + \rho_6)$	0.006
	FMC	WI	0.216	$ND_{2285–2434}$	0.137	0.731	–	–	EVI	0.190	$(\rho_2 - \rho_6) / (0.86 - 1.63)$	0.180
	LAI	MSI/NDMI	0.272	$ND_{2175–2315}$	0.240	0.528	–	–	GVMI	0.288	$\rho_6 / (\rho_2 + \rho_5)$	0.282
	LMA	NDMI	0.002	$ND_{2105–2125}$	0.001	0.004	–	–	GVMI	0.002	$\rho_4 / (\rho_1 + \rho_2)$	0.002
	FB	MSI/NDMI	0.006	$ND_{2175–2315}$	0.005	0.011	–	–	GVMI	0.006	$\rho_6 / (\rho_2 + \rho_5)$	0.006

forests, respectively (Table 8). Grasses benefited most from a fixed soil reducing 37 and 36% of their rRMSE for FWC and CWC, respectively. LMA and FB also reduce their rRMSE to 8 and 5%, respectively. When replacing LMA in the wet samples with those obtained from the site when the sample was dry, using the FMC < 75% threshold, estimations of FMC for the three cover types improved significantly. The method was particularly useful in grasses (RMSE = 0.430) where results are comparable to the improvement obtained when soil is incorporated (RMSE = 0.441), with minor improvements in shrubs (RMSE = 0.89) and far smaller than those obtained when soil is incorporated in forests (RMSE = 0.656). Adding a LAI value to the inversion significantly benefits biochemistry retrievals in forests only, with a larger impact than incorporating the soil. RMSE for FMC is reduced from 0.731 to 0.498. FWC and CWC improve its accuracy to RMSE to 0.006 and 0.009 g/cm^2 whereas if the parameter is free RMSE is equal to 0.009 and 0.012 g/cm^2, respectively. The improvement in rRMSE is of 15% for FWC, 23% for CWC and 24% for FMC.

The MODIS-like RTM inversion using Trombetti et al. (2008) algorithm applied here performs well when retrieving CWC in grasses and shrubs (RMSE = 0.037 and 0.039 g/cm^2, respectively) decaying to a poorer performance in the case of forests (RMSE = 0.1806 g/cm^2).

4. Discussion

4.1. Estimation of water-related variables from field data

One major implication of this study is the potential to calculate FWC and CWC using its relationship with FMC by LMA averaged in time instead of as fresh weight divided by area. Out of the six main water-related variables used in this study, only FMC is not impacted by area

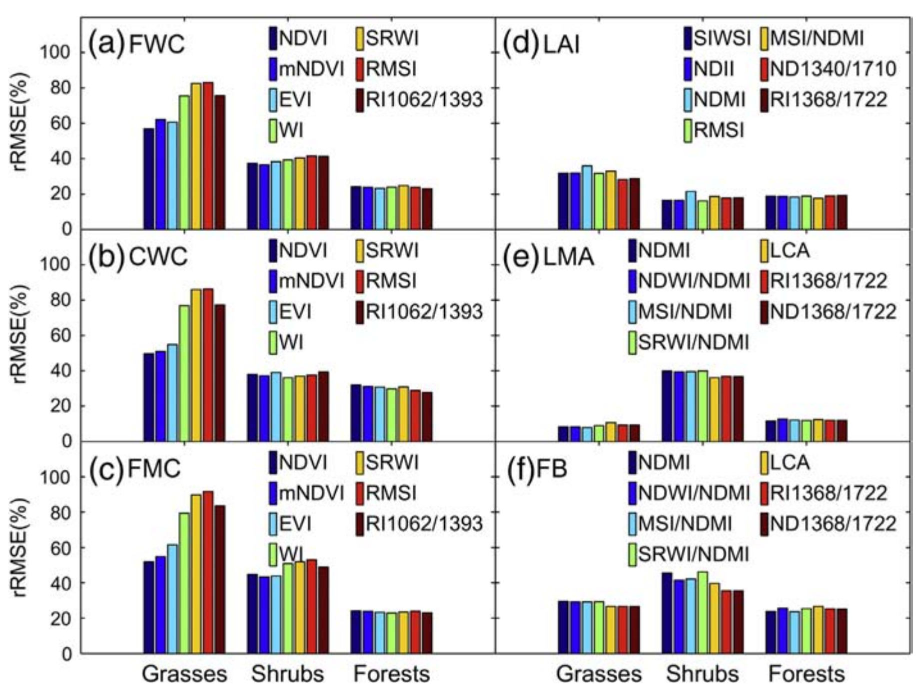

Fig. 4. rRMSE obtained between water-related variables compared with estimations using AVIRIS standard indexes. Only the best performances for each variable are shown.

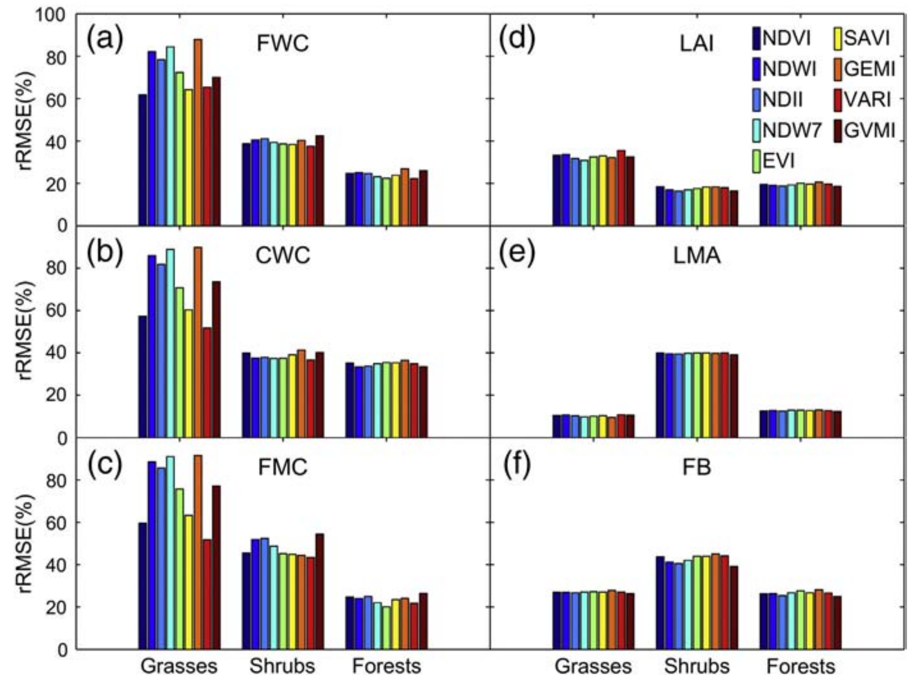

Fig. 5. rRMSE obtained between water-related variables compared with estimations using MODIS standard indexes.

estimations and therefore it is easier to collect (Danson & Bowyer, 2004). However, to quantify FWC and CWC, actual LMA values still must be included in the calculation, even with its own deficiencies, such as lack of representativeness if the sample dataset is not large enough (Ackerly et al., 2002). LMA averaged in time can be derived if it is measured in the experiment or using LMA averaged per species from bibliographic sources if available. The importance of LMA as a leaf trait has promoted the development in recent years of a global database of plant traits (Kattge et al., 2011), which increases the chances to have this data available. This assumption that LMA is time-invariance throughout the year and it is species dependent (Ackerly et al., 2002; Shipley & Vu, 2002) has been previously supported to bypass problems of LMA detection using remote sensing techniques (Chuvieco et al., 2004; Riaño et al., 2005) but not to the knowledge of the authors to improve the representativeness of LMA in FWC and CWC in-situ estimations.

4.2. Curve-fitting techniques

Contrary to previous studies (Cheng et al., 2006; Trombetti et al., 2008), a major conclusion of this work is that it is inadequate to use ACORN CWC or CWC 970 nm to validate water-related retrieval methodologies given that they overestimate CWC in different proportions for each cover type and that RMSE is larger than those obtained with any other method (Table 7). Cheng et al. (2008) evaluated

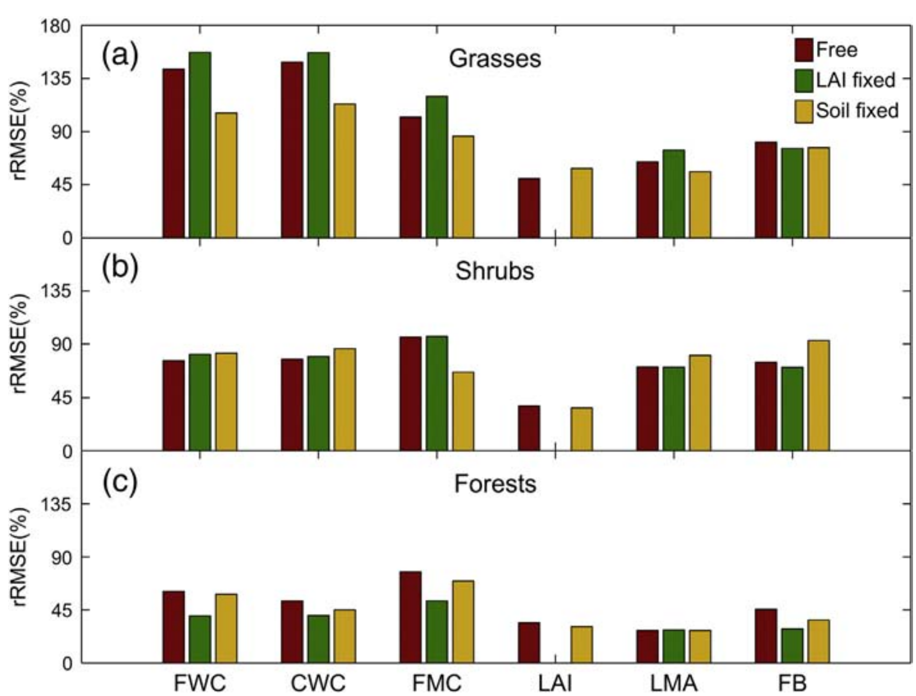

Fig. 6. rRMSE obtained using AVIRIS PROSAIL inversion for a free parameter scenario and LAI and soil fixed scenarios, for each water related variable and cover type.

Table 8
RMSE obtained using AVIRIS PROSAIL inversion with free parameters and LAI and soil fixed scenarios, for each water-related variable and each cover type.

Cover	Variable	Free	LAI fix	Soil fix
Grasses	FWC	0.019	0.021	0.014
	CWC	0.019	0.020	0.015
	FMC	0.524	0.614	0.441
	LAI	0.454	–	0.533
	LMA	0.016	0.019	0.014
	FB	0.017	0.016	0.016
Shrubs	FWC	0.012	0.013	0.013
	CWC	0.018	0.018	0.020
	FMC	0.912	0.917	0.634
	LAI	0.523	–	0.502
	LMA	0.013	0.013	0.015
	FB	0.019	0.019	0.024
Forests	FWC	0.009	0.006	0.008
	CWC	0.012	0.009	0.010
	FMC	0.731	0.498	0.656
	LAI	0.528	–	0.478
	LMA	0.004	0.004	0.004
	FB	0.011	0.007	0.009

MODIS VI against ACORN CWC 940 nm, which was validated with field measurements, finding a good correlation, but also an eight time overestimation. It must be noted that both methods use bands in the NIR where reflectance is dominated by scattering processes instead of absorption (Baret, Vanderbilt, Steven, & Jacquemoud, 1994). Therefore, these would be strongly affected by changes in canopy structure causing the biochemistry to be incorrectly characterized (Knyazikhin et al., 2013). This explanation is reinforced in our study by the fact that this method performs the poorest for forests (larger RMSE) where the structure is most substantial. We infer that overestimation is likely due to multiple scattering (Zhang, Li, & Zhang, 2011) and a correction of the scattering effect is needed if actual CWC values are required (Hunt et al., 2013; Imaging & Geophysics, 2002).

4.3. Standard VI

Segregating per cover type, FWC, CWC and FMC in grasses and shrubs are well retrieved with greenness VI, such as NDVI, mNDVI and EVI (Table 7 and Fig. 4), whereas in forests, where vegetation has more foliage and is denser, NDVI is outperformed by the recently designed $RI_{1062–1393}$ together with other VI with bands in the SWIR such as NDII/NDMI and WI. $RI_{1062–1393}$ works also well in grasses and CWC in shrubs but only in forests it does retrieve FWC in agreement with the performance provided by the authors (Feret et al., 2011). The use of NDVI to retrieve FMC in grasses has been previously reported (Bowyer & Danson, 2004; Chuvieco et al., 2004; Hardy & Burgan, 1999). This is associated with changes in plant chlorophyll content as water diminishes. WI has been used for FMC in previous studies with better results than those obtained in this study (Danson & Bowyer, 2004). Contrary to Al-Moustafa, Armitage, and Danson (2012), MSI was not effective for FMC estimation in shrubs, however it was effective for forests. Noteworthy is the poorer performance of VI to retrieve FWC, CWC, FMC, LMA and FB when all three cover types are combined. This study found a RMSE of 0.013 g/cm^2 and a $R^2 = 0.3$ when NDII retrieves CWC, whereas Hunt et al. (2011) obtained the better value of 0.0091 g/cm^2 and a strong correlation ($R^2 = 0.85$) with a pooled data set of different cover types from different studies. The importance of segregating cover types to retrieve water-related variables that we found in this study has been previously pointed out (Al-Moustafa et al., 2012; Darvishzadeh et al., 2008). This might also be due to the fact that VI is sensitive to the physics of the site conditions (Ustin et al., 2012) and consequently, they lack generality even if the VI has been specifically designed to function over a wide range of physical conditions to try to force its universality (Feret et al., 2011). This reduces the applicability of VI and it is the main reason why physically-based methods are considered better, even though they require parameterization of many input variables and are far more computationally demanding. It must be noted that segregation by cover type is also needed when RTM is applied, which again implies significance of characterizing structure in water related variable retrievals with both methodologies.

VARI and EVI were previously successfully related to FMC (Dennison, Moritz, & Taylor, 2008; Dennison et al., 2005; Roberts et al., 2006; Stow et al., 2005; Yebra et al., 2008). VARI works best for chaparral in this study and across chaparral ecosystems in northern and southern California (Dennison et al., 2008; Stow et al., 2005). We note that contrary to Roberts et al. (2006), VARI retrieved FMC with similar accuracy

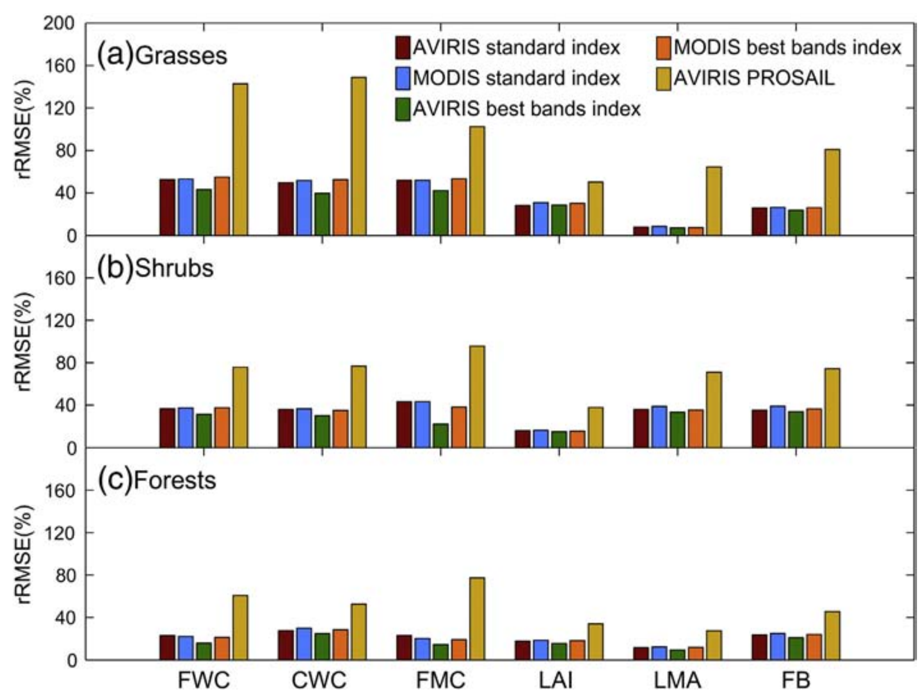

Fig. 7. rRMSE obtained using the best retrieval methods for each water related variable and cover type.

as the best of the AVIRIS standard indexes for grasses and shrubs and significantly outperforming them for forests (Fig. 7). LMA, FB and LAI for shrubs and forests are best retrieved using GVMI even though it was originally designed to retrieve CWC (Ceccato, Flasse, & Gregoire, 2002).

4.4. Best band combination indexes

By using a correlation with the experimental database, FMC was found to have the most remarkable improvement with bands around 2100 nm, 2300 nm and 1700 nm (Table 7). These bands correspond to known absorption features correlated with cellulose and lignin (Curran, 1989; Kokaly et al., 2009), which constitute the main components of the LMA denominator of FMC. LMA also improved its correlation from standard VI using the 1700 nm feature, which was used in the new LMA indexes by Feret et al. (2011) and le Maire et al. (2008). Whereas these indexes relate the band absorption feature at 1700 nm with bands around 1300 nm, our indexes combined the 1700 nm with bands around 1500 nm to obtain better correlations with LMA (Table 7 and Fig. 4). These variations in the wavelengths chosen show the site and species specificity of indexes derived from calibrations with experimental data and the difficulty in designing general across-site indexes to retrieve LMA. Even though a correlation with experimental data is always site dependent and leads to specialized indexes that might perform differently when applied to a wider range of conditions, our results show the importance of longer SWIR bands in the estimation of water-related parameters, particularly FMC, LMA and FB that are still poorly retrieved with standard VI. This result has been pointed out in previous works such as Datt (1999), who found significant correlation with FWC in the SWIR and Bowyer and Danson (2004) for FMC. However, Ceccato et al. (2001) suggested that reflectance in the SWIR only provides information about FWC and not on FMC.

Using best band combination indexes show the potential within the AVIRIS data to improve the retrieval of water related variables together with the importance of the longer wavelength SWIR bands. However, reflected solar radiance is relatively low in this spectral region, resulting in lower signal-to-noise ratio, and atmospheric absorption is significant (Gao, 1996). The development of new and superior quality sensors such as AVIRIS-ng (next generation) have the potential to provide higher precision measurements in this part of the spectrum. In addition, these sensors will make possible the determination of more appropriate absorption coefficients for in-situ biochemical especially in the longer SWIR where water content retrieval is confounded with plant and soil biochemicals (Ustin et al., 2012).

4.5. PROSAIL

Soil background strongly impacts RTM inversion depending on the cover type, especially in grasses and to a lesser extent in forests (Table 8). This result derives from the confounding effect that soil and LMA have in the SWIR (Ceccato et al., 2001; Nagler et al., 2000; Ustin et al., 1998). Constraining the inversion of FWC and particularly LMA to derive FMC with background soil data for any cover type is critical, especially for sparse canopies where light reaches the bare soil within the pixel (Asner, 1998; Huang, Chen, & Cosh, 2009; Jacquemoud, 1993). However, it will not always be possible to find a pure bare soil pixel of all the soil types of interest that are close to the sample site to fix the soil in the RTM inversion (Jacquemoud, 1993). Riaño et al. (2005) method to retrieve FMC was particularly successful in grasses, probably because absorption features associated with LMA are obscured in leaves with higher FWC (Fourty & Baret, 1997), LMA is specific for each species/site (Shipley & Vu, 2002) and LMA at driest stage of the phenological cycle is representative of the annual average LMA (Chuvieco, Aguado, Cocero, & Riaño, 2003). A fixed LAI improved retrieval accuracy in the case of forests. This result indicates the importance of constraining the structural information in the models to retrieve biochemistry using RTM in forests. However, this was not the case for shrubs, which were particularly complicated to characterize, probably due to the mixture of species in each sample site with different LMAs, the variety of soils involved, and a high ratio of non-foliage biomass exposed to the sensor compared to grasses and forests. In addition, it must be mentioned that some shrub sites are in ecotones between soil types, so the soil spectra selected in the model could be erroneous. Retrievals of FMC for shrubs improved by adding the soil reflectance, however the results are far from the 0.15 RMSE provided by Yebra and Chuvieco (2009b) with the incorporation of LAI, but comparable to the accuracy obtained by the authors when no additional selection of LUT combinations is applied. This study found better estimations of LMA than those obtained by Malenovsky et al. (2006) for conifers. CWC retrievals for grasses, shrubs and forests are in the same range as those presented by Bacour, Jacquemoud, Tourbier, Dechambre, and Frangi (2002) and Colombo et al. (2008) for poplar plantations. The best retrievals of FWC are obtained for forests when LAI is fixed and this accuracy is better than the one presented by Kötz et al. (2004).

MODIS-like RTM inversion of CWC using the Trombetti et al. (2008) algorithm performed worse than the one based on AVIRIS and worse than standard VI. This indicates that the inversion does not respond well across sites. Also, it must be noted that for the PROSAIL inversion with MODIS-like data the ranges of FWC, LMA and LAI were not defined using the actual data. These results confirm the complexity of deriving water-related variables through RTM inversion using solely observed data without a precise knowledge and quantification of the physics of the surface (Fourty & Baret, 1997; Jacquemoud et al., 1995). This result is in agreement with previous studies, such as Romero et al. (2012) where LMA in leaves for forest species is accurately estimated only when N, Ca + b and FWC are fixed inputs in the inversion. Similarly, Darvishzadeh, Atzberger, Skidmore, and Schlerf (2011) retrieved LAI for grasses with accuracies comparable to those of statistical approaches, but only with the input of local soil reflectance spectra as a requirement. The main implication of these results is that some parameters may never be completely retrievable on the basis of spectral information alone (Lewis et al., 2012) due to the fact that different combinations of parameters can simulate the same spectral signature, namely equifinality (Kimes, Knyazikhin, Privette, Abuelgasim, & Gao, 2000; Weiss & Baret, 1999). This equifinality is worked around by constraining the model assuming model parameters are invariant in time, a priori knowledge in the form of ancillary measurements, information on canopy architecture or knowledge of the distribution of input canopy variables or even the assumption of known variables set to be fixed values, as it is the case when using VI (Combal et al., 2003; Lewis et al., 2012). Hence, in any inversion from remote sensing observations there will always be a trade-off between the accuracy with which to simulate canopy reflectance with a certain amount of inputs and the maximum number of parameters to retrieve. Finally, it must be noted, that the SAIL model has intrinsic limitations in its capacity to simulate heterogeneous canopies showing clumping at several scales (Jacquemoud et al., 2009). This research shows the importance of LAI on the biochemistry of forests, hence its spectral modeling might be improved by the use of 3D RTM that takes explicitly into account canopy heterogeneity upon the simulations of the radiation regime of scattering and absorption of vegetation. The explicit consideration of structure within a 3D RTM model provides the additional advantage to understand structural influence upon biochemical retrievals (Gastellu-Etchegorry & Bruniquel-Pinel, 2001; Lewis, 2007). Detailed structural measurements of canopies can nowadays be accurately retrieved through methodologies such as radar interferometry or small footprint LiDAR (Lewis, 2007; Ustin, 2013).

4.6. Comparison of methods

A rigorous comparison between CWC_{BB} and FMC_{BB} obtained from the big bags can be done only for grasses, since both variables are calculated from the exact same sample after measuring fresh and dry weights. Fig. 7 shows that whereas AVIRIS PROSAIL inversion retrieves FMC more accurately, VI retrieves CWC and FMC with similar accuracy. This result contradicts previous studies such as Bowyer and Danson (2004) who state in a simulation study that CWC would be more accurate given that it takes into account the effect of spatial and temporal LAI estimations. The fact that VI retrieves CWC better or similarly to FMC might be due to the difficulty in the retrieval of FMC using an index approach for two variables (FWC and LMA), whereas RTM inversion is able to deal with the complexity of the entangled relation between FWC and LMA better and retrieve more accurate FMC values.

In this study, VI retrieved water variables with higher accuracy than inversion methods, particularly when no additional information about the physical conditions of the scene is incorporated to RTM. This result is in agreement with previous works where better results are accomplished when the inversion is constrained with structural data (Meroni, Colombo, & Panigada, 2004; Yebra et al., 2008). It must be noted that index-based methods do not provide a quantification of the biophysical or biochemical variable, and this would be a limiting factor when physical magnitudes are needed. However for applications such as monitoring the state of FMC in vegetation for fire-risk detection, a relative estimation is useful and may be all that is needed (Stow et al., 2005). AVIRIS PROSAIL inversion retrievals of FWC, CWC and FMC are found more accurate than curve-fitting technique results or MODIS CWC PROSAIL inversion for all land cover types.

5. Conclusions

We present an assessment of different methodologies for the retrieval of water related biophysical and biochemical variables in vegetation (FWC, CWC, FMC, LAI, LMA and FB) using AVIRIS and MODIS-like data against ground measurements from three different dates and stratified by three cover types, namely grasses, shrubs and forests. Variables were estimated in different ways using their interrelated properties. Methods tested were: curve-fitting techniques using AVIRIS data, VI, standard and recently designed, best band combination indexes and AVIRIS PROSAIL (this study) and MODIS CWC PROSAIL inversion (Trombetti et al., 2008).

Our results illustrate the complexity of deriving water-related variables using pure RTM inversion approaches across sites without a precise knowledge and quantification of the physics of the surface and the better performance of an index based relationship that neutralizes additional impacts to the spectral signal such as soil background, given the limitations to today's technology and ecological knowledge. RTM simulations were significantly improved with the incorporation of a soil spectrum particularly in the case of grasses and only for LAI in forests. This work also shows the improvement in FMC retrievals using AVIRIS PROSAIL inversion if LMA retrievals from a dry season are assumed earlier in the season, when vegetation has higher water content, particularly for grasses. We show that curve-fitting approaches with water bands on AVIRIS data cannot be used as surrogate truth of CWC to validate water-related variable retrieval methodologies. Our results indicate that there is need to further understand and exploit the longer wavelength SWIR bands, especially for improved retrievals of water related variables by VI, particularly FMC and LMA and FB, that are moderately retrieved with the current generation of standard VI. We find that standard VI retrieves all variables better than any other method. AVIRIS indexes are more accurate than MODIS indexes if best band combinations are used and that AVIRIS standard VI can perform equally or even poorer than MODIS standard VI. This was the case for FMC in forests, where MODIS EVI significantly outperformed AVIRIS EVI. This confirms that there isn't a clear single index that correlates best with each variable, but that different indexes behave differently by both cover type and variable. We also show the possibility to use an averaged LMA over time for estimating FWC and CWC through its relationship with area-independent FMC to overcome possible misrepresentations from ground and areal measurements.

Acknowledgments

This work was supported by funding from the United States National Aeronautics and Space Administration grants #NNG04GQ42G, #NNX11AF93G and #NNX09AN51G. We thank the people of CSTARS at the University of California, Davis for their assistance during the field campaign and especially to Maria Santos for her contribution and Alex Koltunov for his assistance with the pre-processing of the AVIRIS data. We thank the JRBR team for all their support throughout this work; especially to Nona Chiariello. Thanks also go to Dr. Rudolf Richter for his helpful assistance with ATCOR-4. Thanks to Programa de Becas de Movilidad para Profesores Universitarios de la Fundación CajaMadrid which funded Dr. J. Salas' stay at the University of California, Davis.

References

Ackerly, D.D. (2004). Functional strategies of chaparral shrubs in relation to seasonal water deficit and disturbance. *Ecological Monographs*, *74*, 25–44.

Ackerly, D.D., Knight, C. A., Weiss, S. B., Barton, K., & Starmer, K. P. (2002). Leaf size, specific leaf area and microhabitat distribution of chaparral woody plants: Contrasting patterns in species level and community level analyses. *Oecologia*, *130*, 449–457.

Al-Moustafa, T., Armitage, R. P., & Danson, F. M. (2012). Mapping fuel moisture content in upland vegetation using airborne hyperspectral imagery. *Remote Sensing of Environment*, *127*, 74–83.

Asner, G. P. (1998). Biophysical and biochemical sources of variability in canopy reflectance (vol 64, pg 234, 1997). *Remote Sensing of Environment*, *65*, 225–226.

Atzberger, C., Darvishzadeh, R., Schlerf, M., & Le Maire, G. (2013). Suitability and adaptation of PROSAIL radiative transfer model for hyperspectral grassland studies. *Remote Sensing Letters*, *4*, 56–65.

Bacour, C., Jacquemoud, S., Tourbier, Y., Dechambre, M., & Frangi, J. P. (2002). Design and analysis of numerical experiments to compare four canopy reflectance models. *Remote Sensing of Environment*, *79*, 72–83.

Baret, F., & Fourty, T. (1997). Estimation of leaf water content and specific leaf weight from reflectance and transmittance measurements. *Agronomie*, *17*, 455–464.

Baret, F., Vanderbilt, V. C., Steven, M.D., & Jacquemoud, S. (1994). Use of spectral analogy to evaluate canopy reflectance sensitivity to leaf optical properties. *Remote Sensing of Environment*, *48*, 253–260.

Bowyer, P., & Danson, F. M. (2004). Sensitivity of spectral reflectance to variation in live fuel moisture content at leaf and canopy level. *Remote Sensing of Environment*, *92*, 297–308.

Caccamo, G., Chisholm, L. A., Bradstock, R. A., Puotinen, M. L., & Pippen, B. G. (2012). Monitoring live fuel moisture content of heathland, shrubland and sclerophyll forest in south-eastern Australia using MODIS data. *International Journal of Wildland Fire*, *21*, 257–269.

Ceccato, P., Flasse, S., & Gregoire, J. M. (2002). Designing a spectral index to estimate vegetation water content from remote sensing data — Part 2. Validation and applications. *Remote Sensing of Environment*, *82*, 198–207.

Ceccato, P., Flasse, S., Tarantola, S., Jacquemoud, S., & Gregoire, J. M. (2001). Detecting vegetation leaf water content using reflectance in the optical domain. *Remote Sensing of Environment*, *77*, 22–33.

Ceccato, P., Gobron, N., Flasse, S., Pinty, B., & Tarantola, S. (2002). Designing a spectral index to estimate vegetation water content from remote sensing data: Part 1 — Theoretical approach. *Remote Sensing of Environment*, *82*, 188–197.

Champagne, C. M., Staenz, K., Bannari, A., McNairn, H., & Deguise, J. -C. (2003). Validation of a hyperspectral curve-fitting model for the estimation of plant water content of agricultural canopies. *Remote Sensing of Environment*, *87*, 148–160.

Cheng, T., Riaño, D., Koltunov, A., Whiting, M. L., Ustin, S. L., & Rodriguez, J. (2013). Detection of diurnal variation in orchard canopy water content using MODIS/ASTER airborne simulator (MASTER) data. *Remote Sensing of Environment*, *132*, 1–12.

Cheng, Y. -B., Ustin, S. L., Riaño, D., & Vanderbilt, V. C. (2008). Water content estimation from hyperspectral images and MODIS indexes in Southeastern Arizona. *Remote Sensing of Environment*, *112*, 363–374.

Cheng, Y. -B., Zarco-Tejada, P. J., Riaño, D., Rueda, C. A., & Ustin, S. L. (2006). Estimating vegetation water content with hyperspectral data for different canopy scenarios: Relationships between AVIRIS and MODIS indexes. *Remote Sensing of Environment*, *105*, 354–366.

Cho, M.A., Skidmore, A., Corsi, F., van Wieren, S. E., & Sobhan, I. (2007). Estimation of green grass/herb biomass from airborne hyperspectral imagery using spectral indices and partial least squares regression. *International Journal of Applied Earth Observation and Geoinformation*, *9*, 414–424.

Chuvieco, E., Aguado, I., Cocero, D., & Riaño, D. (2003). Design of an empirical index to estimate fuel moisture content from NOAA–AVHRR images in forest fire danger studies. *International Journal of Remote Sensing*, *24*, 1621–1637.

Chuvieco, E., Cocero, D., Riano, D., Martin, P., Martinez-Vega, J., de la Riva, J., et al. (2004). Combining NDVI and surface temperature for the estimation of live fuel moisture content in forest fire danger rating. *Remote Sensing of Environment*, *92*, 322–331.

Coleman, R. G. (2004). Geologic nature of the Jasper Ridge Biological Preserve, San Francisco Peninsula, California. *International Geology Review*, *46*, 629–637.

Colombo, R., Merom, M., Marchesi, A., Busetto, L., Rossini, M., Giardino, C., et al. (2008). Estimation of leaf and canopy water content in poplar plantations by means of hyperspectral indices and inverse modeling. *Remote Sensing of Environment*, *112*, 1820–1834.

Combal, B., Baret, F., Weiss, M., Trubuil, A., Mace, D., Pragnere, A., et al. (2003). Retrieval of canopy biophysical variables from bidirectional reflectance — Using prior information to solve the ill-posed inverse problem. *Remote Sensing of Environment*, *84*, 1–15.

Cornwell, W. K., Schwilk, D. W., & Ackerly, D.D. (2006). A trait-based test for habitat filtering: Convex hull volume. *Ecology*, *87*, 1465–1471.

Cowan, I. R. (1982). Regulation of water use in relation to carbon gain in higher plants. In O. L. Lange, P.S. Nobel, C. B. Osmond, & H. Ziegler (Eds.), *Physiological plant ecology II* (pp. 589–613). Berlin Heidelberg: Springer.

Curcio, J. A., & Petty, C. C. (1951). The near infrared absorption spectrum of liquid water. *JOSA*, *41* (302-302).

Curran, P. J. (1989). Remote sensing of foliar chemistry. *Remote Sensing of Environment*, *30*, 271–278.

Danson, F. M., & Bowyer, P. (2004). Estimating live fuel moisture content from remotely sensed reflectance. *Remote Sensing of Environment*, *92*, 309–321.

Darvishzadeh, R., Atzberger, C., Skidmore, A., & Schlerf, M. (2011). Mapping grassland leaf area index with airborne hyperspectral imagery: A comparison study of statistical approaches and inversion of radiative transfer models. *ISPRS Journal of Photogrammetry and Remote Sensing*, *66*, 894–906.

Darvishzadeh, R., Skidmore, A., Atzberger, C., & van Wieren, S. (2008). Estimation of vegetation LAI from hyperspectral reflectance data: Effects of soil type and plant architecture. *International Journal of Applied Earth Observation and Geoinformation*, *10*, 358–373.

Datt, B. (1999). Remote sensing of water content in *Eucalyptus* leaves. *Australian Journal of Botany*, *47*, 909–923.

Daughtry, C. S. T., Hunt, E. R., Doraiswamy, P. C., & McMurtrey, J. E. (2005). Remote sensing the spatial distribution of crop residues. *Agronomy Journal*, *97*, 864–871.

Dennison, P. E., Moritz, M.A., & Taylor, R. S. (2008). Evaluating predictive models of critical live fuel moisture in the Santa Monica Mountains, California. *International Journal of Wildland Fire*, *17*, 18–27.

Dennison, P. E., Roberts, D. A., Peterson, S. H., & Rechel, J. (2005). Use of normalized difference water index for monitoring live fuel moisture. *International Journal of Remote Sensing*, *26*, 1035–1042.

Dennison, P. E., Roberts, D. A., Thorgusen, S. R., Regelbrugge, J. C., Weise, D., & Lee, C. (2003). Modeling seasonal changes in live fuel moisture and equivalent water thickness using a cumulative water balance index. *Remote Sensing of Environment*, *88*, 442–452.

Fang, H. L., & Liang, S. L. (2003). Retrieving leaf area index with a neural network method: Simulation and validation. *IEEE Transactions on Geoscience and Remote Sensing*, *41*, 2052–2062.

Fensholt, R., & Sandholt, I. (2003). Derivation of a shortwave infrared water stress index from MODIS near- and shortwave infrared data in a semiarid environment. *Remote Sensing of Environment*, *87*, 111–121.

Feret, J. B., & Asner, G. P. (2011). Spectroscopic classification of tropical forest species using radiative transfer modeling. *Remote Sensing of Environment*, *115*, 2415–2422.

Feret, J. B., Francois, C., Gitelson, A., Asner, G. P., Barry, K. M., Panigada, C., et al. (2011). Optimizing spectral indices and chemometric analysis of leaf chemical properties using radiative transfer modeling. *Remote Sensing of Environment*, *115*, 2742–2750.

Fourty, T., & Baret, F. (1997). Vegetation water and dry matter contents estimated from top-of-the-atmosphere reflectance data: A simulation study. *Remote Sensing of Environment*, *61*, 34–45.

Gao, B. -c. (1996). NDWI—A normalized difference water index for remote sensing of vegetation liquid water from space. *Remote Sensing of Environment*, *58*, 257–266.

Gao, B. -C., & Goetzt, A. F. H. (1995). Retrieval of equivalent water thickness and information related to biochemical components of vegetation canopies from AVIRIS data. *Remote Sensing of Environment*, *52*, 155–162.

Garcia, M., Chuvieco, E., Nieto, H., & Aguado, I. (2008). Combining AVHRR and meteorological data for estimating live fuel moisture content. *Remote Sensing of Environment*, *112*, 3618–3627.

Garnier, E., Laurent, G., Bellmann, A., Debain, S., Berthelier, P., Ducout, B., et al. (2001). Consistency of species ranking based on functional leaf traits. *New Phytologist*, *152*, 69–83.

Gastellu-Etchegorry, J. P., & Bruniquel-Pinel, V. (2001). A modeling approach to assess the robustness of spectrometric predictive equations for canopy chemistry. *Remote Sensing of Environment*, *76*, 1–15.

Gitelson, A. A., Kaufman, Y. J., & Merzlyak, M. N. (1996). Use of a green channel in remote sensing of global vegetation from EOS–MODIS. *Remote Sensing of Environment*, *58*, 289–298.

Gitelson, A. A., Kaufman, Y. J., Stark, R., & Rundquist, D. (2002). Novel algorithms for remote estimation of vegetation fraction. *Remote Sensing of Environment*, *80*, 76–87.

Gobron, N., Pinty, B., Verstraete, M. M., & Widlowski, J. L. (2000). Advanced vegetation indices optimized for up-coming sensors: Design, performance, and applications. *IEEE Transactions on Geoscience and Remote Sensing*, *38*, 2489–2505.

Green, R. O., Conel, J. E., & Roberts, D. A. (1993). Estimation of aerosol optical depth, pressure elevation, water vapor, and calculation of apparent surface reflectance from radiance measured by the airborne visible/infrared imaging spectrometer (AVIRIS) using a radiative transfer code. *Optical Engineering and Photonics in Aerospace Sensing* (pp. 2–11). International Society for Optics and Photonics.

Hardisky, M., Klemas, V., & Smart, R. (1983). The influence of soil salinity, growth form, and leaf moisture on the spectral radiance of *Spartina alterniflora* canopies. *Photogrammetric Engineering and Remote Sensing*, *49*, 77–83.

Hardy, C. C., & Burgan, R. E. (1999). Evaluation of NDVI for monitoring live moisture in three vegetation types of the western US. *Photogrammetric Engineering and Remote Sensing*, *65*, 603–610.

Huang, J., Chen, D. Y., & Cosh, M. H. (2009). Sub-pixel reflectance unmixing in estimating vegetation water content and dry biomass of corn and soybeans cropland using normalized difference water index (NDWI) from satellites. *International Journal of Remote Sensing*, *30*, 2075–2104.

Huete, A.R. (1988). A soil-adjusted vegetation index (SAVI). *Remote Sensing of Environment*, *25*, 295–309.

Huete, A., Didan, K., Miura, T., Rodriguez, E. P., Gao, X., & Ferreira, L. G. (2002). Overview of the radiometric and biophysical performance of the MODIS vegetation indices. *Remote Sensing of Environment*, *83*, 195–213.

Hunt, E. R., Li, L., Yilmaz, M. T., & Jackson, T. J. (2011). Comparison of vegetation water contents derived from shortwave-infrared and passive-microwave sensors over central Iowa. *Remote Sensing of Environment*, *115*, 2376–2383.

Hunt, E. R., Jr., & Rock, B. N. (1989). Detection of changes in leaf water content using near- and middle-infrared reflectances. *Remote Sensing of Environment*, *30*, 43–54.

Hunt, E. R., Jr., Ustin, S. L., & Riaño, D. (2013). Remote sensing of leaf, canopy, and vegetation water contents for satellite environmental data records. *Satellite-based Applications on Climate Change* (pp. 335–357). : Springer.

Imaging, A., & Geophysics, L. (2002). ACORN 4.0 user's guide. *Analytical Imaging and Geophysics LLC, Boulder, Colorado*.

Jackson, R. B., Sperry, J. S., & Dawson, T. E. (2000). Root water uptake and transport: Using physiological processes in global predictions. *Trends in Plant Science*, *5*, 482–488.

Jacquemoud, S. (1993). Inversion of the PROSPECT + SAIL canopy reflectance model from AVIRIS equivalent spectra: Theoretical study. *Remote Sensing of Environment*, *44*, 281–292.

Jacquemoud, S., Bacour, C., Poilve, H., & Frangi, J. P. (2000). Comparison of four radiative transfer models to simulate plant canopies reflectance: Direct and inverse mode. *Remote Sensing of Environment*, *74*, 471–481.

Jacquemoud, S., & Baret, F. (1990). PROSPECT: A model of leaf optical properties spectra. *Remote Sensing of Environment*, *34*, 75–91.

Jacquemoud, S., Baret, F., Andrieu, B., Danson, F. M., & Jaggard, K. (1995). Extraction of vegetation biophysical parameters by inversion of the PROSPECT + SAIL models on sugar beet canopy reflectance data. Application to TM and AVIRIS sensors. *Remote Sensing of Environment*, *52*, 163–172.

Jacquemoud, S., Ustin, S. L., Verdebout, J., Schmuck, G., Andreoli, G., & Hosgood, B. (1996). Estimating leaf biochemistry using the PROSPECT leaf optical properties model. *Remote Sensing of Environment*, *56*, 194–202.

Jacquemoud, S., Verhoef, W., Baret, F., Bacour, C., Zarco-Tejada, P. J., Asner, G. P., et al. (2009). PROSPECT plus SAIL models: A review of use for vegetation characterization. *Remote Sensing of Environment*, *113*, S56–S66.

Kattge, J., Diaz, S., Lavorel, S., Prentice, C., Leadley, P., Bonisch, G., et al. (2011). TRY — A global database of plant traits. *Global Change Biology*, *17*, 2905–2935.

Kimes, D. S., Knyazikhin, Y., Privette, J. L., Abuelgasim, A. A., & Gao, F. (2000). Inversion methods for physically-based models. *Remote Sensing Reviews*, *18*, 381–439.

Knyazikhin, Y., Schull, M.A., Stenberg, P., Mottus, M., Rautiainen, M., Yang, Y., et al. (2013). Hyperspectral remote sensing of foliar nitrogen content. *Proceedings of the National Academy of Sciences of the United States of America*, *110*, E185–E192.

Kokaly, R. F., Asner, G. P., Ollinger, S. V., Martin, M. E., & Wessman, C. A. (2009). Characterizing canopy biochemistry from imaging spectroscopy and its application to ecosystem studies. *Remote Sensing of Environment*, *113*, S78–S91.

Kötz, B., Schaepman, M., Morsdorf, F., Bowyer, P., Itten, K., & Allgöwer, B. (2004). Radiative transfer modeling within a heterogeneous canopy for estimation of forest fire fuel properties. *Remote Sensing of Environment*, *92*, 332–344.

Kuusk, A. (1985). The hot spot effect of a uniform vegetation cover. *Soviet Journal of Remote Sensing*, *3*, 646–658.

Kuusk, A. (1991). The hot spot effect in plant canopy reflectance. *Photon–Vegetation Interactions* (pp. 139–159). Springer.

Le Maire, G., François, C., Soudani, K., Berveiller, D., Pontailler, J. Y., Bréda, N., et al. (2008). Calibration and validation of hyperspectral indices for the estimation of broadleaves forest leaf chlorophyll content, leaf mass per area, leaf area index and leaf canopy biomass. *Remote Sensing of Environment*, *112*, 3846–3864.

Lewis, P. (2007). 3D canopy modelling as a tool in remote-sensing research. In J. Vos, L. F. M. Marcelis, P. H. B. de Visser, P. C. Struik, & J. B. Evers (Eds.), *Functional–structural plant modelling in crop production* (pp. 219–229). Springer.

Lewis, P., Gómez-Dans, J., Kaminski, T., Settle, J., Quaife, T., Gobron, N., et al. (2012). An Earth Observation Land Data Assimilation System (EO–LDAS). *Remote Sensing of Environment*, *120*, 219–235.

Li, L., Cheng, Y. B., Ustin, S., Hu, X. T., & Riaño, D. (2008). Retrieval of vegetation equivalent water thickness from reflectance using genetic algorithm (GA)–partial least squares (PLS) regression. *Advances in Space Research*, *41*, 1755–1763.

Malenovsky, Z., Albrechtova, J., Lhotakova, Z., Zurita-Milla, R., Clevers, J., Schaepman, M. E., et al. (2006). Applicability of the PROSPECT model for Norway spruce needles. *International Journal of Remote Sensing*, *27*, 5315–5340.

Meroni, M., Colombo, R., & Panigada, C. (2004). Inversion of a radiative transfer model with hyperspectral observations for LAI mapping in poplar plantations. *Remote Sensing of Environment*, *92*, 195–206.

Mooney, H. A., & Dunn, E. L. (1970). Convergent evolution of Mediterranean-climate evergreen sclerophyll shrubs. *Evolution*, *24*, 292–303.

Nagler, P. L., Daughtry, C. S. T., & Goward, S. N. (2000). Plant litter and soil reflectance. *Remote Sensing of Environment*, *71*, 207–215.

Oze, C., Skinner, C., Schroth, A. W., & Coleman, R. G. (2008). Growing up green on serpentine soils: Biogeochemistry of serpentine vegetation in the Central Coast Range of California. *Applied Geochemistry*, *23*, 3391–3403.

Penuelas, J., Pinol, J., Ogaya, R., & Filella, I. (1997). Estimation of plant water concentration by the reflectance Water Index WI (R900/R970). *International Journal of Remote Sensing*, *18*, 2869–2875.

Peterson, S. H., Roberts, D. A., & Dennison, P. E. (2008). Mapping live fuel moisture with MODIS data: A multiple regression approach. *Remote Sensing of Environment*, *112*, 4272–4284.

Pinty, B., & Verstraete, M. M. (1992). GEMI: A non-linear index to monitor global vegetation from satellites. *Vegetatio*, *101*, 15–20.

Porter, R., & Corelli, T. (2002). *Vascular Plant List*. Jasper Ridge Biological Preserve. California: Stanford University.

Qi, Y., Dennison, P., Spencer, J., & Riaño, D. (2012). Monitoring live fuel moisture using soil moisture and remote sensing proxies. *Fire Ecology*, *8*, 71–87.

Reich, P. B., Ellsworth, D. S., Walters, M. B., Vose, J. M., Gresham, C., Volin, J. C., et al. (1999). Generality of leaf trait relationships: A test across six biomes. *Ecology*, *80*, 1955–1969.

Riaño, D., Vaughan, P., Chuvieco, E., Zarco-Tejada, P. J., & Ustin, S. L. (2005). Estimation of fuel moisture content by inversion of radiative transfer models to simulate equivalent water thickness and dry matter content: Analysis at leaf and canopy level. *IEEE Transactions on Geoscience and Remote Sensing*, *43*, 819–826.

Richter, K., Atzberger, C., Hank, T. B., & Mauser, W. (2012). Derivation of biophysical variables from Earth observation data: Validation and statistical measures. *Journal of Applied Remote Sensing*, *6*.

Richter, R., & Schläpfer, D. (2013). Atmospheric/topographic correction for airborne imagery. *ATCOR-4 user guide version*, *3*.

Roberts, D. A., Dennison, P. E., Peterson, S., Sweeney, S., & Rechel, J. (2006). Evaluation of Airborne Visible/Infrared Imaging Spectrometer (AVIRIS) and Moderate Resolution Imaging Spectrometer (MODIS) measures of live fuel moisture and fuel condition in a shrubland ecosystem in southern California. *Journal of Geophysical Research — Biogeosciences*, *111* (n/a–n/a).

Roberts, D. A., Green, R. O., & Adams, J. B. (1997). Temporal and spatial patterns in vegetation and atmospheric properties from AVIRIS. *Remote Sensing of Environment*, *62*, 223–240.

Romero, A., Aguado, I., & Yebra, M. (2012). Estimation of dry matter content in leaves using normalized indexes and PROSPECT model inversion. *International Journal of Remote Sensing*, *33*, 396–414.

Rouse, J. W., Haas, R. H., Schell, J. A., & Deering, D. W. (1973). *Monitoring vegetation systems in the Great Plains with ERTS*. Third ERTS Symposium, NASA SP-351 I, 309–317.

Rubio, M., Riaño, D., Cheng, Y., & Ustin, S. (2006). Estimation of canopy water content from MODIS using artificial neural networks trained with radiative transfer models. 6th EMS/6th ECAC.

Schlerf, M., & Atzberger, C. (2006). Inversion of a forest reflectance model to estimate structural canopy variables from hyperspectral remote sensing data. *Remote Sensing of Environment*, *100*, 281–294.

Schulze, E. D., & Hall, A. E. (1982). Stomatal responses, water loss and CO_2 assimilation rates of plants in contrasting environments. In O. L. Lange, P.S. Nobel, C. B. Osmond, & H. Ziegler (Eds.), *Physiological plant ecology II* (pp. 181–230). Berlin Heidelberg: Springer.

Shipley, B., & Vu, T. -T. (2002). Dry matter content as a measure of dry matter concentration in plants and their parts. *New Phytologist*, *153*, 359–364.

Sims, D. A., & Gamon, J. A. (2003). Estimation of vegetation water content and photosynthetic tissue area from spectral reflectance: A comparison of indices based on liquid water and chlorophyll absorption features. *Remote Sensing of Environment*, *84*, 526–537.

Stow, D., Niphadkar, M., & Kaiser, J. (2005). MODIS-derived visible atmospherically resistant index for monitoring chaparral moisture content. *International Journal of Remote Sensing*, *26*, 3867–3873.

Stow, D., Niphadkar, M., & Kaiser, J. (2006). Time series of chaparral live fuel moisture maps derived from MODIS satellite data. *International Journal of Wildland Fire*, *15*, 347–360.

Trombetti, M., Riaño, D., Rubio, M.A., Cheng, Y. B., & Ustin, S. L. (2008). Multi-temporal vegetation canopy water content retrieval and interpretation using artificial neural networks for the continental USA. *Remote Sensing of Environment*, *112*, 203–215.

Tucker, C. J. (1979). Red and photographic infrared linear combinations for monitoring vegetation. *Remote Sensing of Environment*, *8*, 127–150.

Ustin, S. L. (2013). Remote sensing of canopy chemistry. *Proceedings of the National Academy of Sciences*, *110*, 804–805.

Ustin, S., Duan, L., Hart, Q., & Haxo, R. (1994). Seasonal changes observed in AVIRIS images of Jasper Ridge, California. *Geoscience and Remote Sensing Symposium, 1994. IGARSS'94. Surface and Atmospheric Remote Sensing: Technologies, Data Analysis and Interpretation, International. IEEE.* (pp. 2360–2362).

Ustin, S. L., Riano, D., & Hunt, E. R. (2012). Estimating canopy water content from spectroscopy. *Israel Journal of Plant Sciences*, *60*, 9–23.

Ustin, S. L., Roberts, D. A., Gamon, J. A., Asner, G. P., & Green, R. O. (2004). Using imaging spectroscopy to study ecosystem processes and properties. *BioScience*, *54*, 523–534.

Ustin, S. L., Roberts, D. A., Pinzón, J., Jacquemoud, S., Gardner, M., Scheer, G., et al. (1998). Estimating canopy water content of chaparral shrubs using optical methods. *Remote Sensing of Environment*, *65*, 280–291.

vanDeventer, A. P., Ward, A.D., Gowda, P. H., & Lyon, J. G. (1997). Using thematic mapper data to identify contrasting soil plains and tillage practices. *Photogrammetric Engineering and Remote Sensing*, *63*, 87–93.

Verhoef, W. (1984). Light scattering by leaf layers with application to canopy reflectance modeling: The SAIL model. *Remote Sensing of Environment*, *16*, 125–141.

Verhoef, W. (1985). Earth observation modeling based on layer scattering matrices. *Remote Sensing of Environment*, *17*, 165–178.

Verhoef, W., & Bach, H. (2007). Coupled soil–leaf-canopy and atmosphere radiative transfer modeling to simulate hyperspectral multi-angular surface reflectance and TOA radiance data. *Remote Sensing of Environment*, *109*, 166–182.

Vohland, M., & Jarmer, T. (2008). Estimating structural and biochemical parameters for grassland from spectroradiometer data by radiative transfer modelling (PROSPECT + SAIL). *International Journal of Remote Sensing*, *29*, 191–209.

Wang, L., Hunt, J. E. R., Qu, J. J., Hao, X., & Daughtry, C. S. T. (2011a). Towards estimation of canopy foliar biomass with spectral reflectance measurements. *Remote Sensing of Environment*, *115*, 836–840.

Wang, L. L., Hunt, E. R., Qu, J. J., Hao, X. J., & Daughtry, C. S. T. (2011b). Estimating dry matter content of fresh leaves from the residuals between leaf and water reflectance. *Remote Sensing Letters*, *2*, 137–145.

Wang, L. L., Hunt, E. R., Qu, J. J., Hao, X. J., & Daughtry, C. S. T. (2013). Remote sensing of fuel moisture content from ratios of narrow-band vegetation water and dry-matter indices. *Remote Sensing of Environment*, *129*, 103–110.

Wang, Q., & Li, P. (2012). Identification of robust hyperspectral indices on forest leaf water content using PROSPECT simulated dataset and field reflectance measurements. *Hydrological Processes*, *26*, 1230–1241.

Weiss, M., & Baret, F. (1999). Evaluation of canopy biophysical variable retrieval performances from the accumulation of large swath satellite data. *Remote Sensing of Environment*, *70*, 293–306.

Wright, I. J., Reich, P. B., Cornelissen, J. H. C., Falster, D. S., Garnier, E., Hikosaka, K., et al. (2005). Assessing the generality of global leaf trait relationships. *New Phytologist*, *166*, 485–496.

Wright, I. J., Reich, P. B., Cornelissen, J. H. C., Falster, D. S., Groom, P. K., Hikosaka, K., et al. (2005). Modulation of leaf economic traits and trait relationships by climate. *Global Ecology and Biogeography*, *14*, 411–421.

Wright, I. J., Reich, P. B., Westoby, M., Ackerly, D.D., Baruch, Z., Bongers, F., et al. (2004). The worldwide leaf economics spectrum. *Nature*, *428*, 821–827.

Yebra, M., & Chuvieco, E. (2009a). Generation of a species-specific look-up table for fuel moisture content assessment. *IEEE Journal of Selected Topics in Applied Earth Observations and Remote Sensing*, *2*, 21–26.

Yebra, M., & Chuvieco, E. (2009b). Linking ecological information and radiative transfer models to estimate fuel moisture content in the Mediterranean region of Spain: Solving the ill-posed inverse problem. *Remote Sensing of Environment*, *113*, 2403–2411.

Yebra, M., Chuvieco, E., & Riano, D. (2008). Estimation of live fuel moisture content from MODIS images for fire risk assessment. *Agricultural and Forest Meteorology*, *148*, 523–536.

Yebra, M., Dennison, P. E., Chuvieco, E., Riaño, D., Zylstra, P., Hunt, E. R., Jr., et al. (2013). A global review of remote sensing of live fuel moisture content for fire danger assessment: Moving towards operational products. *Remote Sensing of Environment*, *136*, 455–468.

Yilmaz, M. T., Hunt, E. R., Jr., Goins, L. D., Ustin, S. L., Vanderbilt, V. C., & Jackson, T. J. (2008). Vegetation water content during SMEX04 from ground data and Landsat 5 Thematic Mapper imagery. *Remote Sensing of Environment*, *112*, 350–362.

Yilmaz, M. T., Hunt, E. R., Jr., & Jackson, T. J. (2008). Remote sensing of vegetation water content from equivalent water thickness using satellite imagery. *Remote Sensing of Environment*, *112*, 2514–2522.

Zarco-Tejada, P. J., Rueda, C. A., & Ustin, S. L. (2003). Water content estimation in vegetation with MODIS reflectance data and model inversion methods. *Remote Sensing of Environment*, *85*, 109–124.

Zhang, Q. X., Li, Q. B., & Zhang, G. J. (2011). Scattering impact analysis and correction for leaf biochemical parameter estimation using Vis-NIR spectroscopy. *Spectroscopy*, *26* (28–+).